Measurement of nuclear effects on ψ(2S) production in p-Pb collisions at √sNN = 8.16 TeV

(ALICE Collaboration) Acharya, S.; ...; Antičić, Tome; ...; Erhardt, Filip; ...; Gotovac, Sven; ...; Jerčić, Marko; ...; ...

Journal article, Published version
Rad u časopisu, Objavljena verzija rada (izdavačev PDF)

Measurement of nuclear effects on $\psi(2S)$ production in p-Pb collisions at $\sqrt{s_{\mathrm{NN}}} = 8.16\,\mathrm{TeV}$

The ALICE collaboration

E-mail: ALICE-publications@cern.ch

ABSTRACT: Inclusive $\psi(2S)$ production is measured in p-Pb collisions at the centre-of-mass energy per nucleon-nucleon pair $\sqrt{s_{\mathrm{NN}}} = 8.16\,\mathrm{TeV}$, using the ALICE detector at the CERN LHC. The production of $\psi(2S)$ is studied at forward ($2.03 < y_{\mathrm{cms}} < 3.53$) and backward ($-4.46 < y_{\mathrm{cms}} < -2.96$) centre-of-mass rapidity and for transverse momentum $p_{\mathrm{T}} < 12\ \mathrm{GeV}/c$ via the decay to muon pairs. In this paper, we report the integrated as well as the y_{cms}- and p_{T}-differential inclusive production cross sections. Nuclear effects on $\psi(2S)$ production are studied via the determination of the nuclear modification factor that shows a strong suppression at both forward and backward centre-of-mass rapidities. Comparisons with corresponding results for inclusive J/ψ show a similar suppression for the two states at forward rapidity (p-going direction), but a stronger suppression for $\psi(2S)$ at backward rapidity (Pb-going direction). As a function of p_{T}, no clear dependence of the nuclear modification factor is found. The relative size of nuclear effects on $\psi(2S)$ production compared to J/ψ is also studied via the double ratio of production cross sections $[\sigma_{\psi(2S)}/\sigma_{\mathrm{J}/\psi}]_{\mathrm{pPb}}/[\sigma_{\psi(2S)}/\sigma_{\mathrm{J}/\psi}]_{\mathrm{pp}}$ between p-Pb and pp collisions. The results are compared with theoretical models that include various effects related to the initial and final state of the collision system and also with previous measurements at $\sqrt{s_{\mathrm{NN}}} = 5.02\,\mathrm{TeV}$.

Contents

1 Introduction

The study of charmonia, bound states of charm (c) and anticharm ($\bar{\text{c}}$) quarks, is an important and interesting research domain. High-energy pp collisions provide a testground to apply quantum chromodynamics (QCD) theory for understanding the charmonium production mechanism. The production of heavy-quark pairs, $c\bar{c}$ in the present case, is an inherently perturbative process since the momentum transfer is at least as large as the heavy-quark pair mass. On the contrary, the formation of the bound state is achieved on a longer time scale and thus has to be considered as a non-perturbative process. QCD-based approaches such as Non-Relativistic QCD (NRQCD) [1] give a good description of the main features of quarkonium production cross sections in pp collisions. When the production of heavy quarkonium occurs inside a medium, as it happens in case of heavy-ion collisions, it is influenced by the properties of the medium and various effects are present. They are mainly categorised in two groups, hot matter effects and cold nuclear matter (CNM) effects. Among the former, those related to the formation of a Quark-Gluon Plasma (QGP), a high energy-density medium created in ultra-relativistic heavy-ion collisions where quarks and gluons are deconfined, are currently scrutinised at collider experiments at RHIC (mainly Au-Au) [2], up to $\sqrt{s_{\text{NN}}} = 0.2\,\text{TeV}$ and the LHC (mainly Pb-Pb) [3–6], up to $\sqrt{s_{\text{NN}}} = 5.02\,\text{TeV}$. For the J/$\psi$ (1S state with J$^{\text{PC}}$ = 1^{--}), a reduced production with respect to pp collisions was reported, ascribed to dissociation in the QGP as a result of color Debye screening [7]. However, LHC experiments reported a significantly reduced suppression for J/ψ with respect to RHIC, now commonly ascribed to a recombination mechanism [8, 9] related to the much larger multiplicity of charm quarks observed at the LHC [10]. When considering the weakly bound ψ(2S) state, Debye screening should lead to a stronger suppression, which at the same time could be influenced by recombination effects. Results currently available at LHC energies on the relative suppression of ψ(2S) and J/ψ [11–13] generally show a stronger effect for the former, except for CMS data on Pb-Pb

collisions at $\sqrt{s_{\mathrm{NN}}} = 2.76\,\mathrm{TeV}$ in the kinematic window $3 < p_{\mathrm{T}} < 30\,\mathrm{GeV/c}$, $1.6 < |y| < 2.4$ where the opposite behaviour was found. Attempts to explain these observations were carried out [14], and it is generally recognised that further precision measurements are needed and might help reaching a final assessment [15].

In addition to more accurate data, a quantitative understanding of the results requires the evaluation of the size of CNM effects, since those are also present in heavy-ion collisions. Among these effects an important role is played by nuclear shadowing [16], the modification of the partonic structure functions inside nuclei. It leads to a change in the probability for a quark or gluon to carry a fraction x of the nucleon momentum and, as a consequence, it affects the production cross section of the $c\bar{c}$ pair. At low x, this effect could originate from the formation of a Color Glass Condensate (CGC) [17], which can happen when, at high energy, the density of low-x quarks and gluons becomes very large, leading to saturation effects. A further mechanism which can also modify the parton kinematics is coherent energy loss, an effect involving partons in the initial and final state [18]. Finally, hadronic/nuclear break-up of the final-state $c\bar{c}$ pair [19] can also occur, and leads to suppression effects. The common way to investigate CNM effects is via proton-nucleus collisions, where hot-matter effects are, in principle, negligible.

Various results on CNM effects on charmonium production are available at LHC energies for p-Pb collisions at $\sqrt{s_{\mathrm{NN}}} = 5.02\,\mathrm{TeV}$. For J/$\psi$, extensive studies were performed at forward/backward centre-of-mass rapidity y_{cms} by ALICE [20–23] and LHCb [24], as well as at midrapidity by ALICE [22], ATLAS [25] and CMS [26]. A general feature of the results is the observation of a significant J/ψ suppression at forward y_{cms} (p-going direction), which becomes weaker and finally disappears moving towards backward rapidity (Pb-going direction). Theory models which include shadowing effects based on various parameterizations of the nuclear modifications of parton distribution functions are able to reproduce the results [27, 28]. At the same time, also models based on a CGC approach [29], or including coherent energy loss as a main CNM mechanism [30], are in good agreement with data. Such an agreement with the models described above also implies that the presence of significant break-up effects of the $c\bar{c}$ pair, which are not included in these models, is disfavoured.

For $\psi(2S)$, results at $\sqrt{s_{\mathrm{NN}}} = 5.02\,\mathrm{TeV}$ [31–35] clearly showed a larger suppression with respect to J/ψ, in particular at backward rapidity. The CNM effects mentioned in the previous paragraph in conjunction with J/ψ results are initial-state effects or anyway directly related to the hard production of the heavy-quark pair, and are expected to affect similarly both charmonium final states. The additional suppression exhibited by the $\psi(2S)$ was therefore attributed to a break-up of this more loosely bound state via collisions with the dense system of interacting particles produced in p-Pb collision [14, 36, 37]. It has to be noted that a similar effect was observed, although with larger uncertainties, by the PHENIX experiment in p-Al and p-Au collisions at $\sqrt{s_{\mathrm{NN}}} = 0.2\,\mathrm{TeV}$ [38].

More recently, with the start of LHC Run 2, p-Pb collisions at $\sqrt{s_{\mathrm{NN}}} = 8.16\,\mathrm{TeV}$ became available. First results on J/ψ, obtained by ALICE [39] and LHCb [40], were compatible within uncertainties with those obtained at $\sqrt{s_{\mathrm{NN}}} = 5.02\,\mathrm{TeV}$. In this paper, we show the first results on inclusive $\psi(2S)$ production in p-Pb collision at $\sqrt{s_{\mathrm{NN}}} = 8.16\,\mathrm{TeV}$.

Section 2 provides a short description of the apparatus and event selection criteria, while the data analysis for $\psi(2S)$ production is described in section 3. Section 4 contains the results, with model comparisons and discussion, and finally a short summary is given in section 5.

2 Experimental apparatus and event selection

Extensive descriptions of the ALICE apparatus and its performance can be found in refs. [41, 42]. The analysis presented in this paper is based on muons detected at forward rapidity with the muon spectrometer [43]. The spectrometer covers the pseudo-rapidity range $-4 < \eta_{\mathrm{lab}} < -2.5$ and includes five tracking stations (Cathode Pad Chambers), the central one embedded inside a dipole magnet with a $3\,\mathrm{T} \cdot \mathrm{m}$ field integral. Each tracking station consists of two tracking chambers aimed at measuring muons in the bending (vertical) and non-bending (horizontal) planes. Two trigger stations (Resistive Plate Chambers), positioned downstream of the tracking system, provide a single muon as well as a dimuon trigger, with a programmable muon p_{T} threshold that was set to $0.5\,\mathrm{GeV}/c$ for this data sample. An absorber, made of concrete, carbon and steel (with a thickness of 10 interaction lengths) is positioned in front of the tracking system, to remove hadrons produced at the interaction vertex. Hadrons which escape this front absorber are further filtered out by a second absorber, placed between the tracking and the triggering system, which also removes low-momentum muons originating from pion and kaon decays, thereby reducing the background. The position of the interaction vertex is determined by the two layers of the Silicon Pixel Detector (SPD) [44], corresponding to the inner part of the ALICE Inner Tracking System (ITS), which cover the pseudo-rapidity intervals $|\eta_{\mathrm{lab}}| < 2$ and $|\eta_{\mathrm{lab}}| < 1.4$. The V0 detector [45], composed of scintillators located at both sides of the interaction point, and covering the pseudo-rapidity intervals $-3.7 < \eta_{\mathrm{lab}} < -1.7$ and $2.8 < \eta_{\mathrm{lab}} < 5.1$, provides the minimum bias trigger. In addition, the V0 is used for luminosity determination, which is also independently estimated by means of the two T0 Cherenkov detectors [46], which cover the pseudo-rapidity intervals $-3.3 < \eta_{\mathrm{lab}} < -3.0$ and $4.6 < \eta_{\mathrm{lab}} < 4.9$.

The data samples were collected with two different beam configurations, which correspond to the acceptance regions $2.03 < y_{\mathrm{cms}} < 3.53$ and $-4.46 < y_{\mathrm{cms}} < -2.96$ for dimuons. These configurations were obtained by reversing the direction of the two beams, and are respectively named p-Pb (forward) and Pb-p (backward) in the following. Positive rapidities correspond to the situation where the proton beam travels towards the muon spectrometer. The integrated luminosities collected for the two configurations are $L_{\mathrm{int}} = 8.4 \pm 0.2\,\mathrm{nb}^{-1}$ for p-Pb and $L_{\mathrm{int}} = 12.8 \pm 0.3\,\mathrm{nb}^{-1}$ for Pb-p collisions [47].

Events selected for this analysis were collected by requiring a coincidence between the minimum bias and the dimuon trigger conditions. In order to reject tracks at the edge of the spectrometer acceptance, the pseudo-rapidity selection $-4 < \eta_{\mu,\mathrm{lab}} < -2.5$ is performed while, to remove tracks crossing the denser regions of the absorber, their radial transverse position (R_{abs}) at the end of the absorber must be in the range $17.6 < R_{\mathrm{abs}} < 89.5$ cm. Finally, the matching based on a χ^2 minimization algorithm between a track in the tracking chambers and a track reconstructed in the trigger system is required.

3 Data analysis

The analysis procedure reported here is similar to the one discussed in refs. [31, 39]. The cross section for inclusive $\psi(2S)$ production times the branching ratio $\text{B.R.}_{\psi(2S)\to\mu^+\mu^-} = (0.80 \pm 0.06)\%$ [48] is given by

$$\text{B.R.}_{\psi(2S)\to\mu^+\mu^-} \cdot \frac{\mathrm{d}^2\sigma_{\text{pPb}}^{\psi(2S)}}{\mathrm{d}p_{\text{T}}\mathrm{d}y} = \frac{N_{\psi(2S)}^{\text{corr}}(y, p_{\text{T}})}{L_{\text{int}} \cdot \Delta y \Delta p_{\text{T}}} \tag{3.1}$$

where $N_{\psi(2S)}^{\text{corr}}(y, p_{\text{T}})$ is the number of $\psi(2S)$ in the corresponding y and p_{T} interval, corrected by the product of acceptance times reconstruction efficiency $A \cdot \epsilon(y, p_{\text{T}})$, L_{int} is the integrated luminosity and Δy, Δp_{T} are the width of the rapidity and transverse momentum intervals. The choice of not correcting for the decay branching ratio is due to the non-negligible systematic uncertainty it would introduce ($\sim 8\%$ [48]).

The number of reconstructed J/ψ and $\psi(2S)$ resonances are extracted via fits to the invariant mass spectrum of opposite-sign muon pairs. More in detail, an extended Crystal Ball function (CB2) [49] is used to describe the shape of the invariant mass signal of the J/ψ and $\psi(2S)$. Alternatively, a pseudo-Gaussian function with a mass-dependent width is also adopted [49]. The background continuum is empirically parameterised either with a Gaussian function with a mass dependent width (VWG) or with a fourth order polynomial times an exponential function, keeping the parameters free in the fit procedure. For J/ψ, the mass and width are also kept as free parameters in the fit, while the other parameters, related to the non-Gaussian tails of the mass shape, are fixed to the values obtained from Monte Carlo (MC) simulations. As a remark, the position of the mass pole of the J/ψ extracted from the fit is in excellent agreement with the PDG value [48] (in most cases within $1\,\text{MeV}/c^2$). As additional tests, the J/ψ tail parameters were either kept free in the fitting procedure, or fixed to those extracted from spectra corresponding to pp collisions at $\sqrt{s} = 8\,\text{TeV}$ [50]. For the $\psi(2S)$, the mass and width are fixed to those of the J/ψ, since the relatively low signal to background ratio does not allow the same approach. The relations that are used are $m_{\psi(2S)} = m_{J/\psi} + m_{\psi(2S)}^{\text{PDG}} - m_{J/\psi}^{\text{PDG}}$ (where $m_{\text{i}}^{\text{PDG}}$ is the mass value from [48]) and $\sigma_{\psi(2S)} = \sigma_{J/\psi} \cdot \sigma_{\psi(2S)}^{\text{MC}}/\sigma_{J/\psi}^{\text{MC}}$, with the latter giving a 5% increase between the J/ψ and $\psi(2S)$ widths. This value is validated using results from a large data sample of pp collisions at $\sqrt{s} = 13\,\text{TeV}$ [51], where the $\psi(2S)$ mass and width are kept free in the fit procedure, and the observed increase between $\sigma_{J/\psi}$ and $\sigma_{\psi(2S)}$ is also 5%. The non-Gaussian tails used for the J/ψ are also adopted for the $\psi(2S)$.

Various fits, combining the options described above were performed, also using two different fit ranges, in order to further test the background description ($2 < m_{\mu\mu} < 5\,\text{GeV}/c^2$ and $2.2 < m_{\mu\mu} < 4.5\,\text{GeV}/c^2$). The raw $\psi(2S)$ yields and their statistical uncertainties are taken to be the average of the results of the various performed fits, while the standard deviation of their distribution is assigned as a systematic uncertainty. An additional 5% uncertainty, corresponding to the uncertainty on the $\psi(2S)$ width in the large pp data sample used to validate the assumption on the relative widths for J/ψ and $\psi(2S)$ [51], is quadratically added.
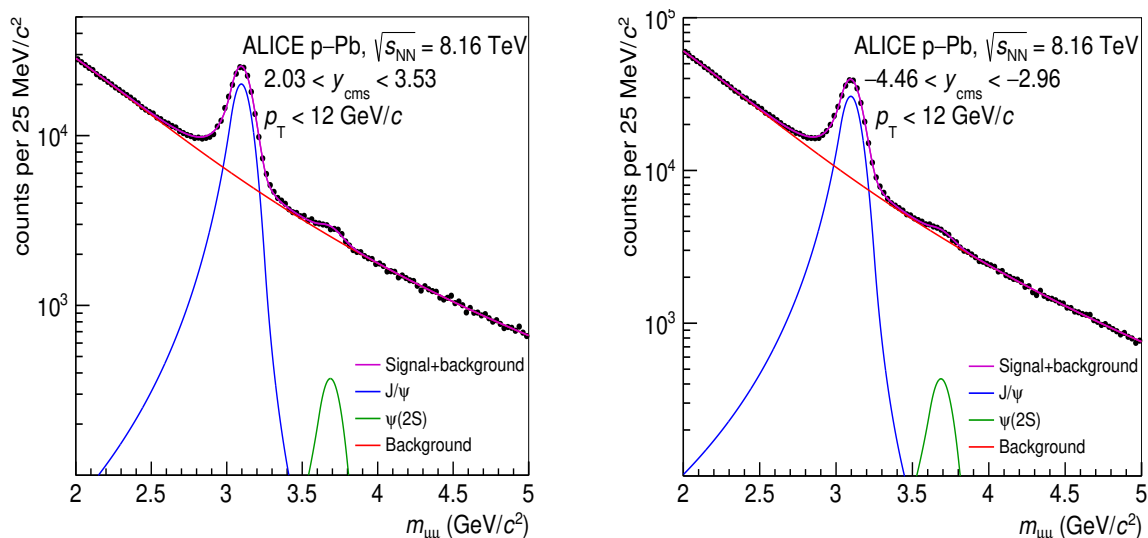
Figure 1. Fit examples of the p_T and y integrated mass spectrum for the forward (left) and backward (right) rapidity data samples. The contribution of the resonances and of the background are also shown separately. These fits are performed using the CB2 as signal function and the VWG background shape.

For the two rapidity intervals under study, the values $N_{\mathrm{pPb}}^{\psi(2\mathrm{S})} = 3148 \pm 253 \pm 243$ and $N_{\mathrm{Pbp}}^{\psi(2\mathrm{S})} = 3595 \pm 283 \pm 368$ were determined, with the first and second uncertainties being statistical and systematic. The measurement is performed in the dimuon pair transverse momentum range $p_T < 12\,\mathrm{GeV}/c$. As an example, figure 1 shows fits to the invariant mass spectra for the two y_{cms} regions. The same procedure is adopted for the evaluation of the differential yields in y_{cms} (2 sub-ranges each for p-Pb and Pb-p) and p_T (5 intervals, up to $p_T = 12\,\mathrm{GeV}/c$). In the interval with largest p_T ($8 < p_T < 12\,\mathrm{GeV}/c$) the raw $\psi(2\mathrm{S})$ yields are $N_{\mathrm{pPb}}^{\psi(2\mathrm{S})} = 150 \pm 39 \pm 30$ and $N_{\mathrm{Pbp}}^{\psi(2\mathrm{S})} = 131 \pm 40 \pm 33$.

The product of acceptance and reconstruction efficiency ($A \cdot \epsilon$) for $\psi(2\mathrm{S})$ is evaluated via MC simulations, performed individually for each run, in order to correctly reproduce the evolution of the detector conditions during data taking. The p_T and y_{cms} input shapes used for the simulation of $\psi(2\mathrm{S})$ are tuned directly on data, by performing a differential analysis in narrower intervals and using an iterative method [39]. The procedure is found to converge after only two iterations. The decay products of the $\psi(2\mathrm{S})$ are then propagated through a realistic description of the ALICE set-up, based on GEANT3.21 [52]. The $A \cdot \epsilon$ values, averaged over the data taking periods and integrated over y_{cms} and p_T, amount to 0.272 for p-Pb and 0.258 for Pb-p collisions, with a negligible statistical uncertainty. The systematic uncertainties on the acceptance are evaluated by performing an alternative simulation based on the corresponding input shapes for the J/ψ [31]. A 3% and 1.5% effect is found for p-Pb and Pb-p, respectively. When considering differential values as a function of y_{cms} and p_T, the uncertainties vary between 0.4–4.0% (0.1–4.4%) for p-Pb (Pb-p). The reconstruction efficiency is the product of trigger, tracking and matching efficiency terms. The latter term refers to the procedure used to pair tracks reconstructed in the tracking

system with the corresponding track segments in the trigger detector. The systematic uncertainties on the three efficiencies mentioned above are evaluated in the same way, and have the same values as those reported for the J/ψ analysis [39]. The largest contribution is that from the trigger which amounts to 2.6% (3.1%) for the integrated p-Pb (Pb-p) data sample.

The integrated luminosities for the two data samples, as detailed in ref. [39], are obtained from $L_{\text{int}} = N_{\text{MB}}/\sigma_{\text{MB}}$, where N_{MB} is the number of MB events and σ_{MB} the cross section corresponding to the MB trigger condition, obtained through a van der Meer scan [47]. The N_{MB} quantity was estimated as the number of analysed dimuon triggers times the inverse of the probability of having a triggered dimuon in a MB event. These values are quoted in ref. [39].

The suppression of $\psi(2S)$ with respect to the corresponding pp yield is quantified by the nuclear modification factor $R_{\text{pPb}}^{\psi(2S)}$. Its evaluation is performed through the following expression:

$$R_{\text{pPb}}^{\psi(2S)}(p_{\text{T}}, y_{\text{cms}}) = \frac{\mathrm{d}^2\sigma_{\text{pPb}}^{\psi(2S)}/\mathrm{d}p_{\text{T}}\mathrm{d}y_{\text{cms}}}{A_{\text{Pb}} \cdot \mathrm{d}^2\sigma_{\text{pp}}^{\psi(2S)}/\mathrm{d}p_{\text{T}}\mathrm{d}y_{\text{cms}}} \tag{3.2}$$

where $A_{\text{Pb}} = 208$ is the mass number of the lead nucleus and the production cross sections in p-Pb and pp are evaluated at the same collision energy and in the same kinematic domain. For this analysis, the $\psi(2S)$ production cross section in pp collisions, integrated over p_{T} and for each of the two rapidity ranges is evaluated from the average of the J/ψ cross sections measured by ALICE [50] and LHCb [53] at $\sqrt{s} = 8\,\text{TeV}$, multiplied by the ratio of cross sections $[\sigma_{\psi(2S)}/\sigma_{\text{J}/\psi}]_{\text{pp}}$, obtained via an interpolation of ALICE results at $\sqrt{s} = 5, 7, 8$ and $13\,\text{TeV}$ [51] assuming no energy dependence. The interpolation is in very good agreement with the pp results, and allows the uncertainties on this quantity to be significantly reduced. To account for the slight difference in collision energy between pp and p-Pb data (8 TeV vs 8.16 TeV) a 1.5% correction factor on the J/ψ cross section at $\sqrt{s} = 8\,\text{TeV}$ is introduced, obtained from an interpolation of J/ψ production cross sections measured at various $\sqrt{s}$ [51]. Finally, both the J/ψ cross section and the $[\sigma^{\psi(2S)}/\sigma^{\text{J}/\psi}]_{\text{pp}}$ ratio must be evaluated in the rapidity domain covered by the p-Pb and Pb-p configurations. For the J/ψ cross section, the procedure detailed in ref. [39] and based on a polynomial or Gaussian interpolation of the y_{cms}-dependence is adopted. For the ratio $[\sigma^{\psi(2S)}/\sigma^{\text{J}/\psi}]_{\text{pp}}$ a small correction factor, related to the slightly different rapidity distributions for J/ψ and $\psi(2S)$, as discussed in ref. [31], and amounting to $\sim 1\%$, is assigned as a systematic uncertainty. Other systematic uncertainties related to $[\sigma^{\psi(2S)}/\sigma^{\text{J}/\psi}]_{\text{pp}}$ include a term (6.0%) corresponding to the uncertainty on the interpolation procedure and a further 1% obtained by assuming, rather than a flat $\sqrt{s}$ dependence of the ratio, the one calculated by NRQCD+CGC models [54, 55] as quoted in ref. [51]. Finally, there is a contribution from the uncertainty on the J/ψ cross section in pp collisions at $\sqrt{s} = 8\,\text{TeV}$ (7.3% for both p-Pb and Pb-p, see table 1 of [39]).

The evaluation of the reference cross section in the rapidity sub-intervals and as a function of p_{T} is performed with the same procedure summarised above. More in detail, for each y_{cms} and p_{T} interval, pp results at various $\sqrt{s}$ are again interpolated with a

source	p-Pb (%)	Pb-p (%)
signal extraction	7.7 (8.0–20.0)	10.2 (9.1–24.9)
trigger efficiency	2.6 (1.0–5.0)	3.1 (1.0–6.0)
tracking efficiency	1.0	2.0
matching efficiency	1.0	1.0
MC input	3 (0.4–4.0)	1.5 (0.1–4.4)
$L_{\mathrm{int}}^{\mathrm{pPb}}$ (corr.)	0.5	0.7
$L_{\mathrm{int}}^{\mathrm{pPb}}$ (uncorr.)	2.1	2.2
pp reference (corr.)	7.1	7.1
pp reference (uncorr.)	6.3 (7.0–11.8)	6.5 (7.2–11.9)

Table 1. Systematic uncertainties on the determination of the $\psi(2S)$ cross sections times branching ratio and nuclear modification factors, shown separately for the p-Pb and Pb-p configurations. When a single value is quoted, it refers to quantities that have no p_{T} or y_{cms} dependence. In the other cases, the number outside parentheses is for integrated quantities, while the ranges in parentheses indicate the variation of the systematic uncertainties in the p_{T} and y_{cms} intervals.

constant function, which is found to well reproduce the data. For this differential study, the relatively small data sample for pp collisions at $\sqrt{s} = 5.02\,\mathrm{TeV}$ [51] is not used in the interpolation.

A summary of the systematic uncertainties on the determination of the $\psi(2S)$ cross sections and of the nuclear modification factor is given in table 1. The contribution from the signal extraction procedure is the largest, and is uncorrelated among the various p_{T} and y_{cms} intervals. The uncertainties on the MC input shapes and on the various efficiencies are also considered as uncorrelated as a function of p_{T} and y_{cms}. The uncertainties on the p-Pb luminosity values correspond to those quoted in ref. [39]. Concerning the pp reference, the uncertainties corresponding to the luminosity measurement affecting the J/ψ cross sections in pp are correlated [39], while the remaining contributions are uncorrelated over y_{cms} and p_{T}. The various uncorrelated and correlated uncertainties are added in quadrature and separately quoted in the numerical results and in the figures of the next section.

4 Results

The measured inclusive $\psi(2S)$ production cross sections for p-Pb collisions at $\sqrt{s_{\mathrm{NN}}} = 8.16\,\mathrm{TeV}$, multiplied by the branching ratio to muon pairs and integrated over $p_{\mathrm{T}} < 12\,\mathrm{GeV}/c$ are:

$$\mathrm{B.R.}_{\cdot\psi(2S)\to\mu^+\mu^-} \cdot \sigma_{\mathrm{pPb}}^{\psi(2S)}(2.03 < y_{\mathrm{cms}} < 3.53) = 1.337 \pm 0.108 \pm 0.121 \pm 0.007\,\mu\mathrm{b}$$

$$\mathrm{B.R.}_{\cdot\psi(2S)\to\mu^+\mu^-} \cdot \sigma_{\mathrm{Pbp}}^{\psi(2S)}(-4.46 < y_{\mathrm{cms}} < -2.96) = 1.124 \pm 0.089 \pm 0.126 \pm 0.008\,\mu\mathrm{b}$$

where the first uncertainty is statistical, the second and third are uncorrelated and correlated systematic, respectively. The differential $\psi(2S)$ cross sections are determined as a
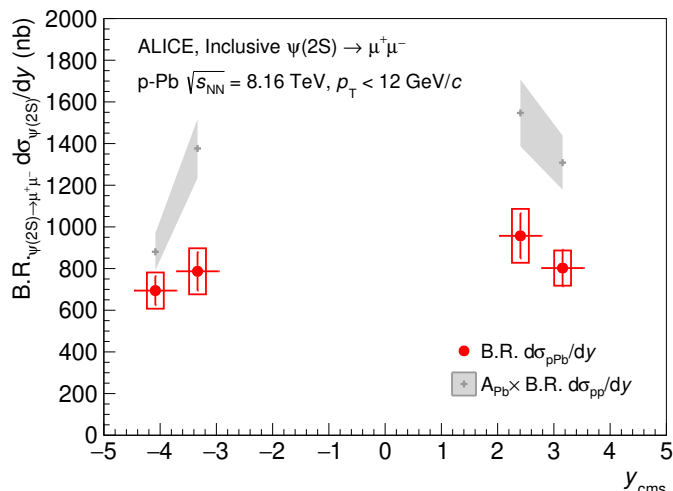
Figure 2. The differential cross section times branching ratio B.R.$_{\psi(2S)\to\mu^+\mu^-}$ d$\sigma^{\psi(2S)}$/dy for $p_{\mathrm{T}} < 12\,\mathrm{GeV}/c$. The error bars represent the statistical uncertainties, while the boxes correspond to total systematic uncertainties. The latter are uncorrelated among the points, except for a very small correlated uncertainty (0.5% and 0.7% for the forward and backward y_{cms} samples, respectively). The grey bands correspond to the reference pp cross section scaled by A_{Pb}.

function of y_{cms} (splitting the forward and backward intervals in two sub-intervals) and p_{T} (5 intervals). The results are shown in figures 2 and 3. The reported values include, in addition to the prompt component, a contribution from the decays of b-hadrons, which was shown by LHCb in p-Pb collisions at $\sqrt{s_{\mathrm{NN}}} = 5.02\,\mathrm{TeV}$ [33] to amount to $\sim$20–30% of the inclusive cross section. Furthermore, figures 2 and 3 also show, as a band, the reference pp cross section obtained with the interpolation procedure described in the previous section, scaled by A_{Pb}.

The ratio of the $\psi(2S)$ and J/ψ cross sections is an interesting quantity for the comparison of the production of the two resonances across different systems, because the terms related to the luminosity and efficiencies and the corresponding uncertainties cancel. It has been computed in this analysis as the ratio of the acceptance-corrected number of $\psi(2S)$ and J/ψ. In figure 4 the p_{T}-integrated cross section ratio is shown for the two rapidity intervals. In the same figure, this quantity is compared with the corresponding pp result at the same collision energy, obtained through the interpolation procedure described in the previous section. At backward rapidity, the ratio is significantly lower (2.9σ effect) than in pp, while at forward rapidity the values are compatible. In the same figure, the results are compared with those obtained in p-Pb collisions at $\sqrt{s_{\mathrm{NN}}} = 5.02\,\mathrm{TeV}$ [31]. No $\sqrt{s_{\mathrm{NN}}}$-dependence can be observed within uncertainties.

In figure 5 the p_{T}-dependence of the ratio of the $\psi(2S)$ and J/ψ cross section is shown. It is compared with the corresponding pp ratio obtained through the interpolation procedure described in the previous section. Also here a stronger relative suppression of $\psi(2S)$ with respect to J/ψ is visible at backward rapidity.

The suppression of $\psi(2S)$ can be more directly quantified by considering the nuclear modification factors, estimated following the procedure described in the previous section.
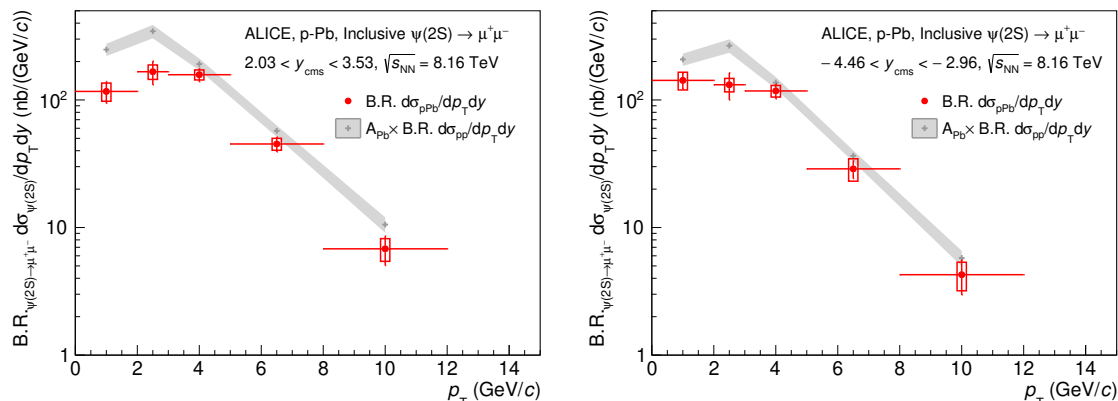
Figure 3. The differential cross sections B.R.$_{\psi(2S)\to\mu^+\mu^-}$d$^2\sigma^{\psi(2S)}$/dydp_T for p-Pb collisions at $\sqrt{s_{NN}}$ = 8.16 TeV, shown separately for the forward and backward y_{cms} samples. The error bars represent the statistical uncertainties, while the boxes correspond to total systematic uncertainties. The latter are uncorrelated among the points, except for a very small correlated uncertainty (0.5% and 0.7% for the forward and backward y_{cms} samples, respectively). The grey bands correspond to the reference pp cross section scaled by A$_{Pb}$.
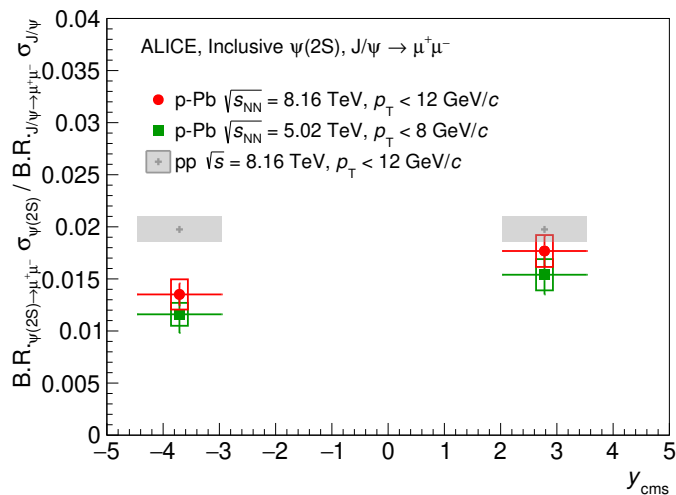
Figure 4. The ratio B.R.$_{\psi(2S)\to\mu^+\mu^-}\sigma^{\psi(2S)}$/B.R.$_{J/\psi\to\mu^+\mu^-}\sigma^{J/\psi}$ as a function of y_{cms} for p-Pb collisions at $\sqrt{s_{NN}}$ = 8.16 TeV, compared with the corresponding pp quantity, shown as a grey band and obtained via an interpolation of results at $\sqrt{s}$ = 5, 7, 8 and 13 TeV [51]. The error bars represent the statistical uncertainties, while the boxes correspond to uncorrelated systematic uncertainties. The published p-Pb results at $\sqrt{s_{NN}}$ = 5.02 TeV [31] are also shown.
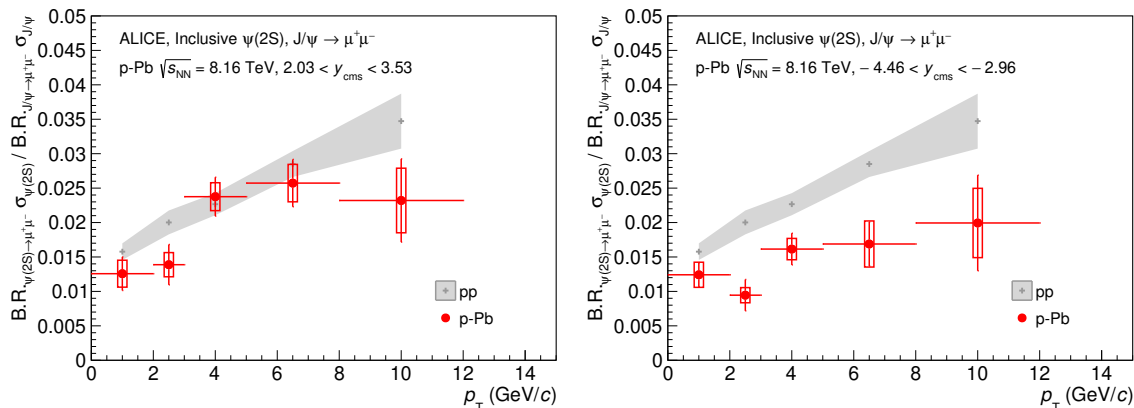
Figure 5. The ratio B.R.$_{\psi(2S)\to\mu^+\mu^-}\sigma^{\psi(2S)}$/B.R.$_{J/\psi\to\mu^+\mu^-}\sigma^{J/\psi}$ as a function of p_T, for p-Pb collisions at $\sqrt{s_{NN}} = 8.16\,\mathrm{TeV}$, compared with the corresponding pp quantity, shown as a grey band and obtained via an interpolation of results at $\sqrt{s} = 7$, 8 and 13 TeV [51]. The error bars represent the statistical uncertainties, while the boxes correspond to uncorrelated systematic uncertainties.

The numerical values, integrated over the interval $p_T < 12\,\mathrm{GeV}/c$, are:

$$R_{\mathrm{pPb}}^{\psi(2S)}(2.03 < y_{\mathrm{cms}} < 3.53) = 0.628 \pm 0.050\,(\mathrm{stat.}) \pm 0.069\,(\mathrm{syst.uncorr.})$$
$$\pm 0.045\,(\mathrm{syst.corr.})$$
$$R_{\mathrm{Pbp}}^{\psi(2S)}(-4.46 < y_{\mathrm{cms}} < -2.96) = 0.684 \pm 0.054\,(\mathrm{stat.}) \pm 0.088\,(\mathrm{syst.uncorr.})$$
$$\pm 0.049\,(\mathrm{syst.corr.})$$

The reported values refer to inclusive production. It was shown by LHCb, when studying p-Pb collisions at $\sqrt{s_{NN}} = 5.02\,\mathrm{TeV}$, that inclusive and prompt nuclear modification factors are compatible within uncertainties [33]. In figure 6, $R_{\mathrm{pPb}}^{\psi(2S)}$ is shown splitting the forward and backward rapidity samples in two intervals. The results are compared with those for $R_{\mathrm{pPb}}^{J/\psi}$ [39]. For $\psi(2S)$, the suppression reaches up to 30–40% and is compatible, within uncertainties, at forward and backward y_{cms}. Relatively to J/ψ, a stronger suppression is visible at backward rapidity, whereas the results are compatible at forward rapidity. The data are also compared (left panel) with theoretical calculations based on initial-state effects or coherent energy loss, whose output is largely independent on the specific charmonium resonance, and can therefore be compared with both J/ψ and $\psi(2S)$ results. Calculations based on the CGC approach [56, 57], on nuclear shadowing [57, 58], implemented according to different parameterizations (EPS09NLO [59], nCTEQ15 [60]) or finally on coherent energy loss [57, 61], show good agreement with the J/ψ results but fail to describe the $\psi(2S)$ R_{pPb} at backward rapidity.

The possible influence of final-state interactions, leading to a break-up of the charmonium resonances, is taken into account in theory calculations where these effects are due to either soft color exchanges in the hadronizing $c\bar{c}$ pair [36], or final-state interactions with the comoving medium [37]. The former calculation describes the initial state in terms of a CGC state, and results are available only at forward rapidity, corresponding to low Bjorken-x values in the Pb nucleus, where the system may be described using this
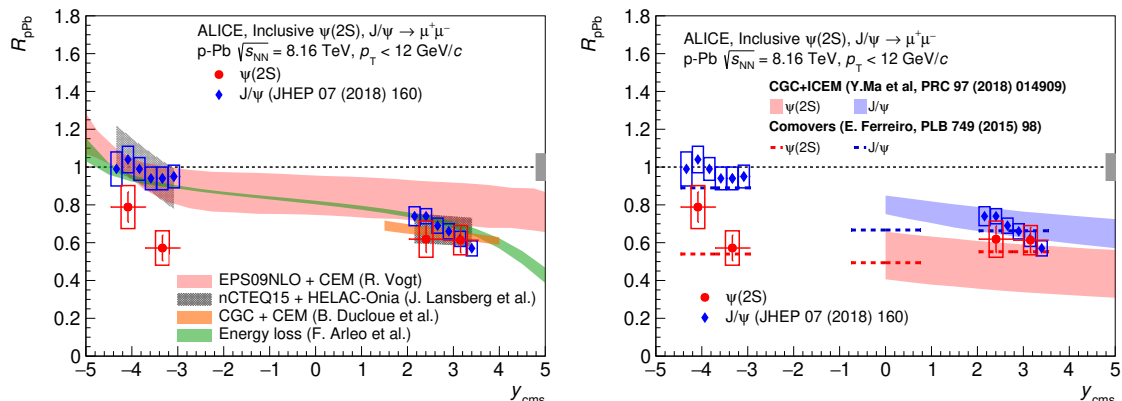
Figure 6. The y_{cms}-dependence of R_{pPb} for $\psi(2S)$ and J/ψ [39] in p-Pb collisions at $\sqrt{s_{NN}} = 8.16$ TeV. The error bars represent the statistical uncertainties, while the boxes correspond to uncorrelated systematic uncertainties and the box at $R_{pPb} = 1$ to correlated systematic uncertainties. The results are compared with models including initial-state effects [56–58] and coherent energy loss [57, 61] (left panel), and to models which also implement final-state effects [36, 37] (right panel).
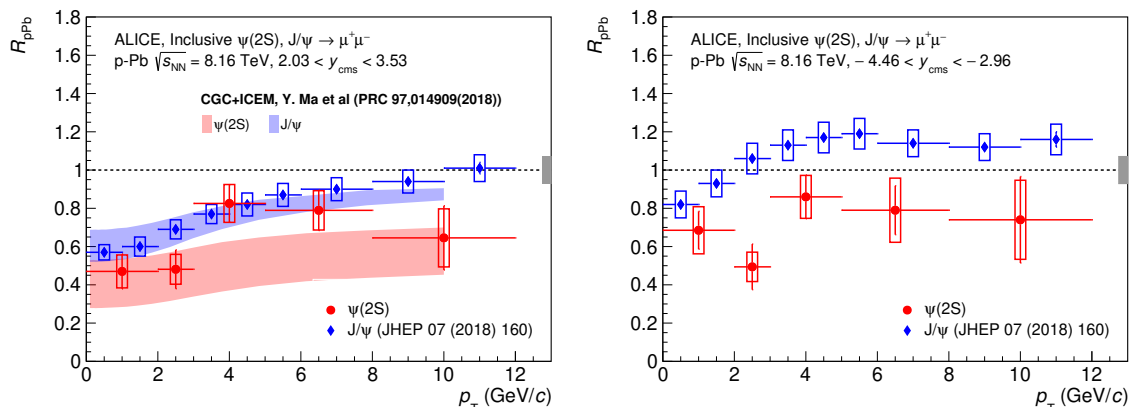
Figure 7. The p_T-dependence of R_{pPb} for $\psi(2S)$ and J/ψ at forward (left) and backward (right) rapidity in p-Pb collisions, at $\sqrt{s_{NN}} = 8.16$ TeV. The error bars represent the statistical uncertainties, while the boxes correspond to uncorrelated systematic uncertainties and the box at $R_{pPb} = 1$ to correlated systematic uncertainties. The comparison with the results of a CGC-based model [36], which implements final-state effects, is also shown.

approach. The two models reach a fair agreement with data for both $\psi(2S)$ and J/ψ, as shown in the right panel of figure 6.

The present data sample allows a p_T-differential study of $R_{pPb}^{\psi(2S)}$ up to $p_T = 12$ GeV/c. The results are plotted in figure 7, separately for forward and backward rapidity, and compared with published results for J/ψ [39]. At forward rapidity the $\psi(2S)$ suppression is compatible with that of J/ψ, while at backward rapidity the $\psi(2S)$ suppression, which is independent of p_T within uncertainties, is significantly stronger. The CGC-based model [36] results are found to fairly match the experimental findings. No theory comparison is yet available for backward rapidity.
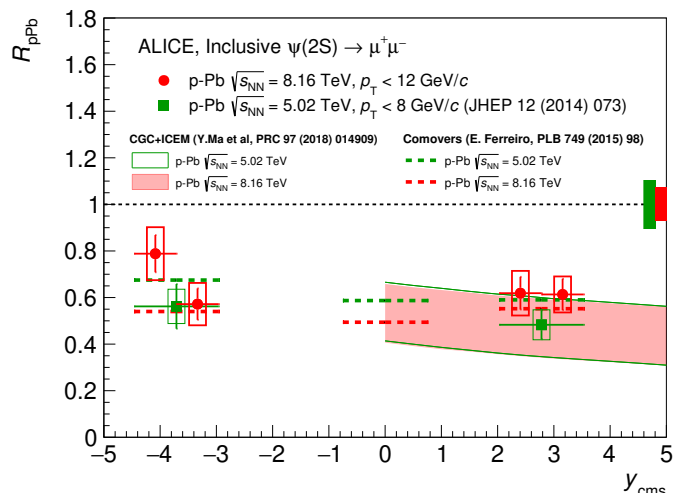
Figure 8. Comparison of the rapidity dependence of R_{pPb} for $\psi(2S)$ in p-Pb collisions at $\sqrt{s_{\mathrm{NN}}} = 8.16$ and $5.02\,\mathrm{TeV}$ [31]. The error bars represent the statistical uncertainties, while the boxes correspond to uncorrelated systematic uncertainties and the boxes at $R_{\mathrm{pPb}} = 1$ to correlated systematic uncertainties, separately shown for the two energies. The results are also compared with theoretical models that include final-state effects [36, 37].

In figure 8, a comparison of the rapidity dependence of $\psi(2S)$ suppression at $\sqrt{s_{\mathrm{NN}}} = 8.16\,\mathrm{TeV}$ and $5.02\,\mathrm{TeV}$ [39] is presented, together with the corresponding results from theoretical models which implement final-state effects [36, 37]. Both models fairly describe the $\psi(2S)$ nuclear modification factor at both energies. The data at the two energies are in agreement within uncertainties. In ref. [31], the reference for the $\psi(2S)$ R_{pPb} evaluation at $\sqrt{s_{\mathrm{NN}}} = 5.02\,\mathrm{TeV}$ was based only on the $\sqrt{s} = 7\,\mathrm{TeV}$ pp data available at that time [62]. If the procedure described in this paper would be adopted for the $\sqrt{s_{\mathrm{NN}}} = 5.02\,\mathrm{TeV}$ result, the reference pp cross section would be lower by 12% (corresponding to 0.9σ on that quantity) and the R_{pPb} values would therefore be higher by the same amount. In any case, the slightly stronger suppression predicted at $\sqrt{s_{\mathrm{NN}}} = 8.16\,\mathrm{TeV}$ and backward rapidity in refs. [37, 57], related to the larger density of produced particles at higher energy, is beyond the sensitivity of the current measurement.

In figure 9, the results on the p_{T}-dependence of $R_{\mathrm{pPb}}^{\psi(2S)}$ at the two energies studied by ALICE are presented. Within uncertainties, there is a fair agreement between the results, without a clear indication of a p_{T}-dependence, except possibly for the backward-rapidity results at $\sqrt{s_{\mathrm{NN}}} = 5.02\,\mathrm{TeV}$ which show a tendency to an increase at high p_{T}.

Finally, also to ease comparisons with future results from other experiments, we present in figure 10, as a function of y_{cms} and figure 11, as a function of p_{T}, the values of the double ratio of the $\psi(2S)$ and J/ψ cross sections between p-Pb and pp. Clearly, these results confirm the features observed when comparing the nuclear modification factors for the two resonances, i.e., the y_{cms}-dependence shows a relative suppression of the $\psi(2S)$ with respect to the J/ψ at backward rapidity, while the p_{T}-dependence does not indicate a clear trend.
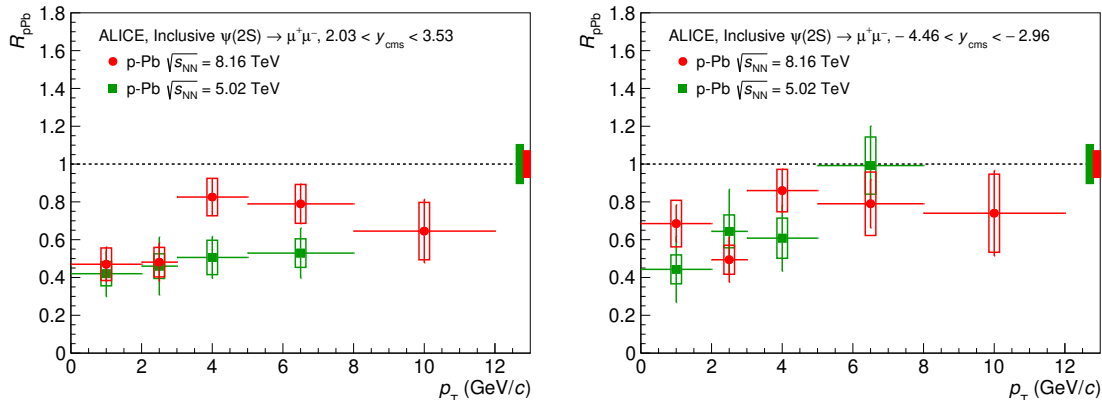
Figure 9. Comparison of the transverse-momentum dependence of R_{pPb} for $\psi(2S)$ in p-Pb collisions at $\sqrt{s_{\mathrm{NN}}} = 8.16$ and $5.02\,\mathrm{TeV}$ [31]. The error bars represent the statistical uncertainties, while the boxes correspond to uncorrelated systematic uncertainties and the boxes at $R_{\mathrm{pPb}} = 1$ to correlated systematic uncertainties, separately shown for the two energies.
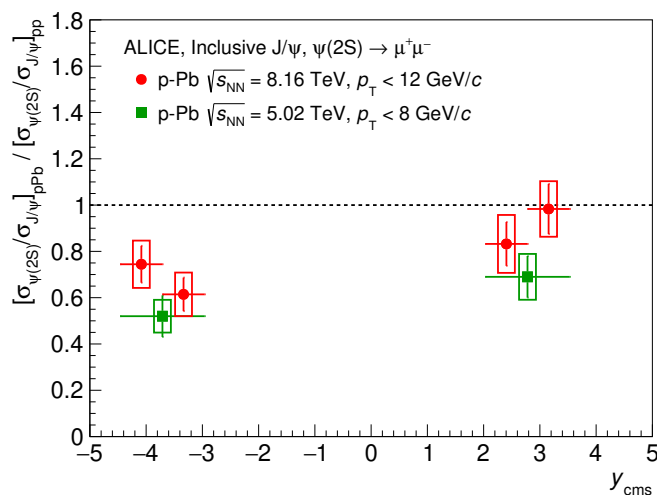
Figure 10. Double ratio of $\psi(2S)$ and J/ψ cross sections in p-Pb and pp collisions as a function of rapidity, at $\sqrt{s_{\mathrm{NN}}} = 8.16\,\mathrm{TeV}$, compared with the corresponding results at $\sqrt{s_{\mathrm{NN}}} = 5.02\,\mathrm{TeV}$ [31]. The error bars represent the statistical uncertainties, while the boxes correspond to uncorrelated systematic uncertainties.

5 Conclusions

The results of studies on the inclusive $\psi(2S)$ production in p-Pb collisions at $\sqrt{s_{\mathrm{NN}}} = 8.16\,\mathrm{TeV}$, performed by ALICE, were shown. The data sample is about two times larger than the one at $\sqrt{s_{\mathrm{NN}}} = 5.02\,\mathrm{TeV}$, which was the object of a previous analysis [39].

The values of the nuclear modification factor indicate a 30–40% $\psi(2S)$ suppression at both forward and backward rapidity, with no significant transverse momentum dependence. When compared with the corresponding values for J/ψ, a similar suppression is found at forward rapidity, likely dominated by initial-state effects such as nuclear shadowing. At
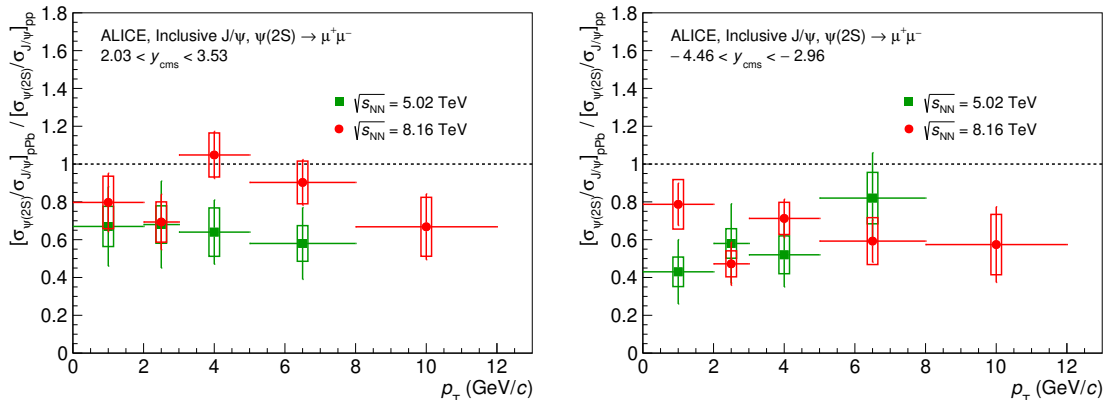
Figure 11. Double ratio of $\psi(2S)$ and J/ψ cross sections in p-Pb and pp collisions as a function of transverse momentum, at forward (left) and backward (right) rapidity at $\sqrt{s_{NN}} = 8.16$ TeV, compared with the corresponding results at $\sqrt{s_{NN}} = 5.02$ TeV [31]. The error bars represent the statistical uncertainties, while the boxes correspond to uncorrelated systematic uncertainties.

backward rapidity, the $\psi(2S)$ suppression is significantly stronger than that of J/ψ. This effect is well reproduced by theoretical models that complement initial-state with final-state break-up effects, which should be more important for the loosely bound $\psi(2S)$ state. These results also confirm, with a better accuracy and extending the p_T reach, the previous observations carried out by ALICE in p-Pb collisions at $\sqrt{s_{NN}} = 5.02$ TeV.

Acknowledgments

References

[1] G.T. Bodwin, E. Braaten and G. Lepage, *Rigorous QCD analysis of inclusive annihilation and production of heavy quarkonium*, *Phys. Rev. D* **51** (1995) 1125 [*Erratum ibid.* **55** (1997) 5853] [hep-ph/9407339] [INSPIRE].

[2] STAR collaboration, *Measurement of inclusive J/ψ suppression in Au+Au collisions at √s_NN = 200 GeV through the dimuon channel at STAR*, *Phys. Lett. B* **797** (2019) 134917 [arXiv:1905.13669] [INSPIRE].

[3] ALICE collaboration, *J/ψ suppression at forward rapidity in Pb-Pb collisions at √s_NN = 5.02 TeV*, *Phys. Lett. B* **766** (2017) 212 [arXiv:1606.08197] [INSPIRE].

[4] ALICE collaboration, *Centrality and transverse momentum dependence of inclusive J/ψ production at midrapidity in Pb-Pb collisions at √s_NN = 5.02 TeV*, *Phys. Lett. B* **805** (2020) 135434 [arXiv:1910.14404] [INSPIRE].

[5] CMS collaboration, *Measurement of prompt and nonprompt charmonium suppression in PbPb collisions at 5.02 TeV*, *Eur. Phys. J. C* **78** (2018) 509 [arXiv:1712.08959] [INSPIRE].

[6] ATLAS collaboration, *Prompt and non-prompt J/ψ and ψ(2S) suppression at high transverse momentum in 5.02 TeV Pb+Pb collisions with the ATLAS experiment*, *Eur. Phys. J. C* **78** (2018) 762 [arXiv:1805.04077] [INSPIRE].

[7] T. Matsui and H. Satz, *J/ψ Suppression by Quark-Gluon Plasma Formation*, *Phys. Lett. B* **178** (1986) 416 [INSPIRE].

[8] P. Braun-Munzinger and J. Stachel, *(Non)thermal aspects of charmonium production and a new look at J/ψ suppression*, *Phys. Lett. B* **490** (2000) 196 [nucl-th/0007059] [INSPIRE].

[9] R.L. Thews, M. Schroedter and J. Rafelski, *Enhanced J/ψ production in deconfined quark matter*, *Phys. Rev. C* **63** (2001) 054905 [hep-ph/0007323] [INSPIRE].

[10] ALICE collaboration, *D-meson production in p-Pb collisions at √s_NN = 5.02 TeV and in pp collisions at √s = 7 TeV*, *Phys. Rev. C* **94** (2016) 054908 [arXiv:1605.07569] [INSPIRE].

[11] CMS collaboration, *Measurement of Prompt ψ(2S) → J/ψ Yield Ratios in Pb-Pb and p − p Collisions at √s_NN = 2.76 TeV*, *Phys. Rev. Lett.* **113** (2014) 262301 [arXiv:1410.1804] [INSPIRE].

[12] CMS collaboration, *Relative Modification of Prompt ψ(2S) and J/ψ Yields from pp to PbPb Collisions at √s_NN = 5.02 TeV*, *Phys. Rev. Lett.* **118** (2017) 162301 [arXiv:1611.01438] [INSPIRE].

[13] ALICE collaboration, *Differential studies of inclusive J/ψ and ψ(2S) production at forward rapidity in Pb-Pb collisions at √s_NN = 2.76 TeV*, *JHEP* **05** (2016) 179 [arXiv:1506.08804] [INSPIRE].

[14] X. Du and R. Rapp, *Sequential Regeneration of Charmonia in Heavy-Ion Collisions*, *Nucl. Phys. A* **943** (2015) 147 [arXiv:1504.00670] [INSPIRE].

[15] A. Dainese, M. Mangano, A.B. Meyer, A. Nisati, G. Salam and M.A. Vesterinen, *Report on the Physics at the HL-LHC, and Perspectives for the HE-LHC*, Tech. Rep. CERN-2019-007, Geneva, Switzerland (2019), DOI.

[16] K.J. Eskola, P. Paakkinen, H. Paukkunen and C.A. Salgado, *EPPS16: Nuclear parton distributions with LHC data*, *Eur. Phys. J. C* **77** (2017) 163 [arXiv:1612.05741] [INSPIRE].

[17] F. Gelis, E. Iancu, J. Jalilian-Marian and R. Venugopalan, *The Color Glass Condensate*, *Ann. Rev. Nucl. Part. Sci.* **60** (2010) 463 [arXiv:1002.0333] [INSPIRE].

[18] F. Arleo and S. Peignè, *J/ψ suppression in p-A collisions from parton energy loss in cold QCD matter*, *Phys. Rev. Lett.* **109** (2012) 122301 [arXiv:1204.4609] [INSPIRE].

[19] D.C. McGlinchey, A.D. Frawley and R. Vogt, *Impact parameter dependence of the nuclear modification of J/ψ production in d+Au collisions at $\sqrt{s_{NN}} = 200\,GeV$*, *Phys. Rev. C* **87** (2013) 054910 [arXiv:1208.2667] [INSPIRE].

[20] ALICE collaboration, *J/ψ production and nuclear effects in p-Pb collisions at $\sqrt{s_{NN}} = 5.02\,TeV$*, *JHEP* **02** (2014) 073 [arXiv:1308.6726] [INSPIRE].

[21] ALICE collaboration, *Centrality dependence of inclusive J/ψ production in p-Pb collisions at $\sqrt{s_{NN}} = 5.02\,TeV$*, *JHEP* **11** (2015) 127 [arXiv:1506.08808] [INSPIRE].

[22] ALICE collaboration, *Rapidity and transverse-momentum dependence of the inclusive J/ψ nuclear modification factor in p-Pb collisions at $\sqrt{s_{NN}} = 5.02\,TeV$*, *JHEP* **06** (2015) 055 [arXiv:1503.07179] [INSPIRE].

[23] ALICE collaboration, *J/ψ production as a function of charged-particle pseudorapidity density in p-Pb collisions at $\sqrt{s_{NN}} = 5.02\,TeV$*, *Phys. Lett. B* **776** (2018) 91 [arXiv:1704.00274] [INSPIRE].

[24] LHCb collaboration, *Study of J/ψ production and cold nuclear matter effects in pPb collisions at $\sqrt{s_{NN}} = 5\,TeV$*, *JHEP* **02** (2014) 072 [arXiv:1308.6729] [INSPIRE].

[25] ATLAS collaboration, *Measurement of differential J/ψ production cross sections and forward-backward ratios in p + Pb collisions with the ATLAS detector*, *Phys. Rev. C* **92** (2015) 034904 [arXiv:1505.08141] [INSPIRE].

[26] CMS collaboration, *Measurement of prompt and nonprompt J/ψ production in pp and pPb collisions at $\sqrt{s_{NN}} = 5.02\,TeV$*, *Eur. Phys. J. C* **77** (2017) 269 [arXiv:1702.01462] [INSPIRE].

[27] J.L. Albacete et al., *Predictions for p+Pb Collisions at $\sqrt{s_{NN}} = 5\,TeV$*, *Int. J. Mod. Phys. E* **22** (2013) 1330007 [arXiv:1301.3395] [INSPIRE].

[28] J.-P. Lansberg and H.-S. Shao, *Towards an automated tool to evaluate the impact of the nuclear modification of the gluon density on quarkonium, D and B meson production in proton-nucleus collisions*, *Eur. Phys. J. C* **77** (2017) 1 [arXiv:1610.05382] [INSPIRE].

[29] Y.-Q. Ma, R. Venugopalan and H.-F. Zhang, *J/ψ production and suppression in high energy proton-nucleus collisions*, *Phys. Rev. D* **92** (2015) 071901 [arXiv:1503.07772] [INSPIRE].

[30] F. Arleo, R. Kolevatov, S. Peigné and M. Rustamova, *Centrality and pT dependence of J/psi suppression in proton-nucleus collisions from parton energy loss*, *JHEP* **05** (2013) 155 [arXiv:1304.0901] [INSPIRE].

[31] ALICE collaboration, *Suppression of ψ(2S) production in p-Pb collisions at $\sqrt{s_{NN}} = 5.02\,TeV$*, *JHEP* **12** (2014) 073 [arXiv:1405.3796] [INSPIRE].

[32] ALICE collaboration, *Centrality dependence of ψ(2S) suppression in p-Pb collisions at $\sqrt{s_{NN}} = 5.02\,TeV$*, *JHEP* **06** (2016) 050 [arXiv:1603.02816] [INSPIRE].

[33] LHCb collaboration, *Study of ψ(2S) production and cold nuclear matter effects in pPb collisions at $\sqrt{s_{NN}} = 5\,TeV$*, *JHEP* **03** (2016) 133 [arXiv:1601.07878] [INSPIRE].

[34] CMS collaboration, *Measurement of prompt ψ(2S) production cross sections in proton-lead and proton-proton collisions at* $\sqrt{s_{\mathrm{NN}}} = 5.02$ *TeV*, *Phys. Lett. B* **790** (2019) 509 [arXiv:1805.02248] [INSPIRE].

[35] ATLAS collaboration, *Measurement of quarkonium production in proton-lead and proton-proton collisions at* 5.02 TeV *with the ATLAS detector*, *Eur. Phys. J. C* **78** (2018) 171 [arXiv:1709.03089] [INSPIRE].

[36] Y.-Q. Ma, R. Venugopalan, K. Watanabe and H.-F. Zhang, *ψ(2S) versus J/ψ suppression in proton-nucleus collisions from factorization violating soft color exchanges*, *Phys. Rev. C* **97** (2018) 014909 [arXiv:1707.07266] [INSPIRE].

[37] E.G. Ferreiro, *Excited charmonium suppression in proton-nucleus collisions as a consequence of comovers*, *Phys. Lett. B* **749** (2015) 98 [arXiv:1411.0549] [INSPIRE].

[38] PHENIX collaboration, *Measurement of the relative yields of ψ(2S) to ψ(1S) mesons produced at forward and backward rapidity in p+p, p+Al, p+Au, and* ^{3}He+Au *collisions at* $\sqrt{s_{\mathrm{NN}}} = 200$ *GeV*, *Phys. Rev. C* **95** (2017) 034904 [arXiv:1609.06550] [INSPIRE].

[39] ALICE collaboration, *Inclusive J/ψ production at forward and backward rapidity in p-Pb collisions at* $\sqrt{s_{\mathrm{NN}}} = 8.16$ *TeV*, *JHEP* **07** (2018) 160 [arXiv:1805.04381] [INSPIRE].

[40] LHCb collaboration, *Prompt and nonprompt J/ψ production and nuclear modification in pPb collisions at* $\sqrt{s_{\mathrm{NN}}} = 8.16$ *TeV*, *Phys. Lett. B* **774** (2017) 159 [arXiv:1706.07122] [INSPIRE].

[41] ALICE collaboration, *The ALICE experiment at the CERN LHC*, 2008 *JINST* **3** S08002 [INSPIRE].

[42] ALICE collaboration, *Performance of the ALICE Experiment at the CERN LHC*, *Int. J. Mod. Phys. A* **29** (2014) 1430044 [arXiv:1402.4476] [INSPIRE].

[43] ALICE collaboration, *Rapidity and transverse momentum dependence of inclusive J/ψ production in pp collisions at* $\sqrt{s} = 7$ *TeV*, *Phys. Lett. B* **704** (2011) 442 [*Erratum ibid.* **718** (2012) 692] [arXiv:1105.0380] [INSPIRE].

[44] ALICE collaboration, *Alignment of the ALICE Inner Tracking System with cosmic-ray tracks*, 2010 *JINST* **5** P03003 [arXiv:1001.0502] [INSPIRE].

[45] ALICE collaboration, *Performance of the ALICE VZERO system*, 2013 *JINST* **8** P10016 [arXiv:1306.3130] [INSPIRE].

[46] M. Bondila et al., *ALICE T0 detector*, *IEEE Trans. Nucl. Sci.* **52** (2005) 1705.

[47] ALICE collaboration, *ALICE luminosity determination for p-Pb collisions at* $\sqrt{s_{\mathrm{NN}}} = 8.16$ *TeV*, ALICE-PUBLIC-2018-002.

[48] PARTICLE DATA GROUP collaboration, *Review of Particle Physics*, *Phys. Rev. D* **98** (2018) 030001 [INSPIRE].

[49] ALICE collaboration, *Quarkonium signal extraction in ALICE*, ALICE-PUBLIC-2015-006.

[50] ALICE collaboration, *Inclusive quarkonium production at forward rapidity in pp collisions at* $\sqrt{s} = 8$ *TeV*, *Eur. Phys. J. C* **76** (2016) 184 [arXiv:1509.08258] [INSPIRE].

[51] ALICE collaboration, *Energy dependence of forward-rapidity* J/ψ *and ψ(2S) production in pp collisions at the LHC*, *Eur. Phys. J. C* **77** (2017) 392 [arXiv:1702.00557] [INSPIRE].

[52] R. Brun et al., *GEANT: Detector Description and Simulation Tool; Oct 1994*, CERN Program Library, CERN, Geneva (1993).

[53] LHCb collaboration, *Production of J/ψ and Υ mesons in pp collisions at √s = 8 TeV*, *JHEP* **06** (2013) 064 [arXiv:1304.6977] [INSPIRE].

[54] Y.-Q. Ma, K. Wang and K.-T. Chao, *J/ψ(ψ′) production at the Tevatron and LHC at $\mathcal{O}(\alpha_s^4 v^4)$ in nonrelativistic QCD*, *Phys. Rev. Lett.* **106** (2011) 042002 [arXiv:1009.3655] [INSPIRE].

[55] Y.-Q. Ma and R. Venugopalan, *Comprehensive Description of J/ψ Production in Proton-Proton Collisions at Collider Energies*, *Phys. Rev. Lett.* **113** (2014) 192301 [arXiv:1408.4075] [INSPIRE].

[56] B. Ducloué, T. Lappi and H. Mäntysaari, *Forward J/ψ production at high energy: centrality dependence and mean transverse momentum*, *Phys. Rev. D* **94** (2016) 074031 [arXiv:1605.05680] [INSPIRE].

[57] J.L. Albacete et al., *Predictions for Cold Nuclear Matter Effects in p+Pb Collisions at $\sqrt{s_{NN}}$ = 8.16 TeV*, *Nucl. Phys. A* **972** (2018) 18 [arXiv:1707.09973] [INSPIRE].

[58] A. Kusina, J.-P. Lansberg, I. Schienbein and H.-S. Shao, *Gluon Shadowing in Heavy-Flavor Production at the LHC*, *Phys. Rev. Lett.* **121** (2018) 052004 [arXiv:1712.07024] [INSPIRE].

[59] K.J. Eskola, H. Paukkunen and C.A. Salgado, *EPS09: A New Generation of NLO and LO Nuclear Parton Distribution Functions*, *JHEP* **04** (2009) 065 [arXiv:0902.4154] [INSPIRE].

[60] K. Kovarik et al., *nCTEQ15 — Global analysis of nuclear parton distributions with uncertainties in the CTEQ framework*, *Phys. Rev. D* **93** (2016) 085037 [arXiv:1509.00792] [INSPIRE].

[61] F. Arleo and S. Peigné, *Quarkonium suppression in heavy-ion collisions from coherent energy loss in cold nuclear matter*, *JHEP* **10** (2014) 073 [arXiv:1407.5054] [INSPIRE].

[62] ALICE collaboration, *Measurement of quarkonium production at forward rapidity in pp collisions at √s = 7 TeV*, *Eur. Phys. J. C* **74** (2014) 2974 [arXiv:1403.3648] [INSPIRE].

The ALICE collaboration

S. Acharya[141], D. Adamová[95], A. Adler[74], J. Adolfsson[81], M.M. Aggarwal[100], G. Aglieri Rinella[34], M. Agnello[30], N. Agrawal[10,54], Z. Ahammed[141], S. Ahmad[16], S.U. Ahn[76], A. Akindinov[92], M. Al-Turany[107], S.N. Alam[141], D.S.D. Albuquerque[122], D. Aleksandrov[88], B. Alessandro[59], H.M. Alfanda[6], R. Alfaro Molina[71], B. Ali[16], Y. Ali[14], A. Alici[10,26,54], A. Alkin[2], J. Alme[21], T. Alt[68], L. Altenkamper[21], I. Altsybeev[113], M.N. Anaam[6], C. Andrei[48], D. Andreou[34], H.A. Andrews[111], A. Andronic[144], M. Angeletti[34], V. Anguelov[104], C. Anson[15], T. Antičić[108], F. Antinori[57], P. Antonioli[54], N. Apadula[80], L. Aphecetche[115], H. Appelshäuser[68], S. Arcelli[26], R. Arnaldi[59], M. Arratia[80], I.C. Arsene[20], M. Arslandok[104], A. Augustinus[34], R. Averbeck[107], S. Aziz[78], M.D. Azmi[16], A. Badalà[56], Y.W. Baek[41], S. Bagnasco[59], X. Bai[107], R. Bailhache[68], R. Bala[101], A. Balbino[30], A. Baldisseri[137], M. Ball[43], S. Balouza[105], D. Banerjee[3], R. Barbera[27], L. Barioglio[25], G.G. Barnaföldi[145], L.S. Barnby[94], V. Barret[134], P. Bartalini[6], K. Barth[34], E. Bartsch[68], F. Baruffaldi[28], N. Bastid[134], S. Basu[143], G. Batigne[115], B. Batyunya[75], D. Bauri[49], J.L. Bazo Alba[112], I.G. Bearden[89], C. Beattie[146], C. Bedda[63], N.K. Behera[61], I. Belikov[136], A.D.C. Bell Hechavarria[144], F. Bellini[34], R. Bellwied[125], V. Belyaev[93], G. Bencedi[145], S. Beole[25], A. Bercuci[48], Y. Berdnikov[98], D. Berenyi[145], R.A. Bertens[130], D. Berzano[59], M.G. Besoiu[67], L. Betev[34], A. Bhasin[101], I.R. Bhat[101], M.A. Bhat[3], H. Bhatt[49], B. Bhattacharjee[42], A. Bianchi[25], L. Bianchi[25], N. Bianchi[52], J. Bielčík[37], J. Bielčíková[95], A. Bilandzic[105], G. Biro[145], R. Biswas[3], S. Biswas[3], J.T. Blair[119], D. Blau[88], C. Blume[68], G. Boca[139], F. Bock[34,96], A. Bogdanov[93], S. Boi[23], L. Boldizsár[145], A. Bolozdynya[93], M. Bombara[38], G. Bonomi[140], H. Borel[137], A. Borissov[93], H. Bossi[146], E. Botta[25], L. Bratrud[68], P. Braun-Munzinger[107], M. Bregant[121], M. Broz[37], E. Bruna[59], G.E. Bruno[106], M.D. Buckland[127], D. Budnikov[109], H. Buesching[68], S. Bufalino[30], O. Bugnon[115], P. Buhler[114], P. Buncic[34], Z. Buthelezi[72,131], J.B. Butt[14], J.T. Buxton[97], S.A. Bysiak[118], D. Caffarri[90], A. Caliva[107], E. Calvo Villar[112], R.S. Camacho[45], P. Camerini[24], A.A. Capon[114], F. Carnesecchi[10,26], R. Caron[137], J. Castillo Castellanos[137], A.J. Castro[130], E.A.R. Casula[55], F. Catalano[30], C. Ceballos Sanchez[53], P. Chakraborty[49], S. Chandra[141], W. Chang[6], S. Chapeland[34], M. Chartier[127], S. Chattopadhyay[141], S. Chattopadhyay[110], A. Chauvin[23], C. Cheshkov[135], B. Cheynis[135], V. Chibante Barroso[34], D.D. Chinellato[122], S. Cho[61], P. Chochula[34], T. Chowdhury[134], P. Christakoglou[90], C.H. Christensen[89], P. Christiansen[81], T. Chujo[133], C. Cicalo[55], L. Cifarelli[10,26], F. Cindolo[54], G. Clai[54,ii], J. Cleymans[124], F. Colamaria[53], D. Colella[53], A. Collu[80], M. Colocci[26], M. Concas[59,iii], G. Conesa Balbastre[79], Z. Conesa del Valle[78], G. Contin[24,60], J.G. Contreras[37], T.M. Cormier[96], Y. Corrales Morales[25], P. Cortese[31], M.R. Cosentino[123], F. Costa[34], S. Costanza[139], P. Crochet[134], E. Cuautle[69], P. Cui[6], L. Cunqueiro[96], D. Dabrowski[142], T. Dahms[105], A. Dainese[57], F.P.A. Damas[115,137], M.C. Danisch[104], A. Danu[67], D. Das[110], I. Das[110], P. Das[86], P. Das[3], S. Das[3], A. Dash[86], S. Dash[49], S. De[86], A. De Caro[29], G. de Cataldo[53], J. de Cuveland[39], A. De Falco[23], D. De Gruttola[10], N. De Marco[59], S. De Pasquale[29], S. Deb[50], H.F. Degenhardt[121], K.R. Deja[142], A. Deloff[85], S. Delsanto[25,131], W. Deng[6], D. Devetak[107], P. Dhankher[49], D. Di Bari[33], A. Di Mauro[34], R.A. Diaz[8], T. Dietel[124], P. Dillenseger[68], Y. Ding[6], R. Divià[34], D.U. Dixit[19], Ø. Djuvsland[21], U. Dmitrieva[62], A. Dobrin[67], B. Dönigus[68], O. Dordic[20], A.K. Dubey[141], A. Dubla[107], S. Dudi[100], M. Dukhishyam[86], P. Dupieux[134], R.J. Ehlers[96,146], V.N. Eikeland[21], D. Elia[53], E. Epple[146], B. Erazmus[115], F. Erhardt[99], A. Erokhin[113], M.R. Ersdal[21], B. Espagnon[78], G. Eulisse[34], D. Evans[111], S. Evdokimov[91], L. Fabbietti[105], M. Faggin[28], J. Faivre[79], F. Fan[6], A. Fantoni[52], M. Fasel[96], P. Fecchio[30], A. Feliciello[59], G. Feofilov[113], A. Fernández Téllez[45], A. Ferrero[137], A. Ferretti[25], A. Festanti[34], V.J.G. Feuillard[104], J. Figiel[118], S. Filchagin[109], D. Finogeev[62], F.M. Fionda[21], G. Fiorenza[53], F. Flor[125], S. Foertsch[72], P. Foka[107], S. Fokin[88], E. Fragiacomo[60],

U. Frankenfeld[107], U. Fuchs[34], C. Furget[79], A. Furs[62], M. Fusco Girard[29], J.J. Gaardhøje[89], M. Gagliardi[25], A.M. Gago[112], A. Gal[136], C.D. Galvan[120], P. Ganoti[84], C. Garabatos[107], E. Garcia-Solis[11], K. Garg[115], C. Gargiulo[34], A. Garibli[87], K. Garner[144], P. Gasik[105], E.F. Gauger[119], M.B. Gay Ducati[70], M. Germain[115], J. Ghosh[110], P. Ghosh[141], S.K. Ghosh[3], M. Giacalone[26], P. Gianotti[52], P. Giubellino[59,107], P. Giubilato[28], P. Glässel[104], A. Gomez Ramirez[74], V. Gonzalez[107,143], L.H. González-Trueba[71], S. Gorbunov[39], L. Görlich[118], A. Goswami[49], S. Gotovac[35], V. Grabski[71], L.K. Graczykowski[142], K.L. Graham[111], L. Greiner[80], A. Grelli[63], C. Grigoras[34], V. Grigoriev[93], A. Grigoryan[1], S. Grigoryan[75], O.S. Groettvik[21], F. Grosa[30], J.F. Grosse-Oetringhaus[34], R. Grosso[107], R. Guernane[79], M. Guittiere[115], K. Gulbrandsen[89], T. Gunji[132], A. Gupta[101], R. Gupta[101], I.B. Guzman[45], R. Haake[146], M.K. Habib[107], C. Hadjidakis[78], H. Hamagaki[82], G. Hamar[145], M. Hamid[6], R. Hannigan[119], M.R. Haque[63,86], A. Harlenderova[107], J.W. Harris[146], A. Harton[11], J.A. Hasenbichler[34], H. Hassan[96], D. Hatzifotiadou[10,54], P. Hauer[43], S. Hayashi[132], S.T. Heckel[68,105], E. Hellbär[68], H. Helstrup[36], A. Herghelegiu[48], T. Herman[37], E.G. Hernandez[45], G. Herrera Corral[9], F. Herrmann[144], K.F. Hetland[36], H. Hillemanns[34], C. Hills[127], B. Hippolyte[136], B. Hohlweger[105], J. Honermann[144], D. Horak[37], A. Hornung[68], S. Hornung[107], R. Hosokawa[15], P. Hristov[34], C. Huang[78], C. Hughes[130], P. Huhn[68], T.J. Humanic[97], H. Hushnud[110], L.A. Husova[144], N. Hussain[42], S.A. Hussain[14], D. Hutter[39], J.P. Iddon[34,127], R. Ilkaev[109], H. Ilyas[14], M. Inaba[133], G.M. Innocenti[34], M. Ippolitov[88], A. Isakov[95], M.S. Islam[110], M. Ivanov[107], V. Ivanov[98], V. Izucheev[91], B. Jacak[80], N. Jacazio[34], P.M. Jacobs[80], S. Jadlovska[117], J. Jadlovsky[117], S. Jaelani[63], C. Jahnke[121], M.J. Jakubowska[142], M.A. Janik[142], T. Janson[74], M. Jercic[99], O. Jevons[111], M. Jin[125], F. Jonas[96,144], P.G. Jones[111], J. Jung[68], M. Jung[68], A. Jusko[111], P. Kalinak[64], A. Kalweit[34], V. Kaplin[93], S. Kar[6], A. Karasu Uysal[77], O. Karavichev[62], T. Karavicheva[62], P. Karczmarczyk[34], E. Karpechev[62], U. Kebschull[74], R. Keidel[47], M. Keil[34], B. Ketzer[43], Z. Khabanova[90], A.M. Khan[6], S. Khan[16], S.A. Khan[141], A. Khanzadeev[98], Y. Kharlov[91], A. Khatun[16], A. Khuntia[118], B. Kileng[36], B. Kim[61], B. Kim[133], D. Kim[147], D.J. Kim[126], E.J. Kim[73], H. Kim[17,147], J. Kim[147], J.S. Kim[41], J. Kim[104], J. Kim[147], J. Kim[73], M. Kim[104], S. Kim[18], T. Kim[147], T. Kim[147], S. Kirsch[68], I. Kisel[39], S. Kiselev[92], A. Kisiel[142], J.L. Klay[5], C. Klein[68], J. Klein[34,59], S. Klein[80], C. Klein-Bösing[144], M. Kleiner[68], A. Kluge[34], M.L. Knichel[34], A.G. Knospe[125], C. Kobdaj[116], M.K. Köhler[104], T. Kollegger[107], A. Kondratyev[75], N. Kondratyeva[93], E. Kondratyuk[91], J. Konig[68], P.J. Konopka[34], G. Kornakov[142], L. Koska[117], O. Kovalenko[85], V. Kovalenko[113], M. Kowalski[118], I. Králik[64], A. Kravčáková[38], L. Kreis[107], M. Krivda[64,111], F. Krizek[95], K. Krizkova Gajdosova[37], M. Krüger[68], E. Kryshen[98], M. Krzewicki[39], A.M. Kubera[97], V. Kučera[34,61], C. Kuhn[136], P.G. Kuijer[90], L. Kumar[100], S. Kundu[86], P. Kurashvili[85], A. Kurepin[62], A.B. Kurepin[62], A. Kuryakin[109], S. Kushpil[95], J. Kvapil[111], M.J. Kweon[61], J.Y. Kwon[61], Y. Kwon[147], S.L. La Pointe[39], P. La Rocca[27], Y.S. Lai[80], R. Langoy[129], K. Lapidus[34], A. Lardeux[20], P. Larionov[52], E. Laudi[34], R. Lavicka[37], T. Lazareva[113], R. Lea[24], L. Leardini[104], J. Lee[133], S. Lee[147], F. Lehas[90], S. Lehner[114], J. Lehrbach[39], R.C. Lemmon[94], I. León Monzón[120], E.D. Lesser[19], M. Lettrich[34], P. Lévai[145], X. Li[12], X.L. Li[6], J. Lien[129], R. Lietava[111], B. Lim[17], V. Lindenstruth[39], A. Lindner[48], S.W. Lindsay[127], C. Lippmann[107], M.A. Lisa[97], A. Liu[19], J. Liu[127], S. Liu[97], W.J. Llope[143], I.M. Lofnes[21], V. Loginov[93], C. Loizides[96], P. Loncar[35], J.A. Lopez[104], X. Lopez[134], E. López Torres[8], J.R. Luhder[144], M. Lunardon[28], G. Luparello[60], Y.G. Ma[40], A. Maevskaya[62], M. Mager[34], S.M. Mahmood[20], T. Mahmoud[43], A. Maire[136], R.D. Majka[146,i], M. Malaev[98], Q.W. Malik[20], L. Malinina[75,iv], D. Mal'Kevich[92], P. Malzacher[107], G. Mandaglio[32,56], V. Manko[88], F. Manso[134], V. Manzari[53], Y. Mao[6], M. Marchisone[135], J. Mareš[66], G.V. Margagliotti[24], A. Margotti[54], J. Margutti[63], A. Marín[107], C. Markert[119], M. Marquard[68], C.D. Martin[24], N.A. Martin[104], P. Martinengo[34], J.L. Martinez[125],

M.I. Martínez[45], G. Martínez García[115], S. Masciocchi[107], M. Masera[25], A. Masoni[55],
L. Massacrier[78], E. Masson[115], A. Mastroserio[53,138], A.M. Mathis[105], O. Matonoha[81],
P.F.T. Matuoka[121], A. Matyja[118], C. Mayer[118], F. Mazzaschi[25], M. Mazzilli[53], M.A. Mazzoni[58],
A.F. Mechler[68], F. Meddi[22], Y. Melikyan[62,93], A. Menchaca-Rocha[71], C. Mengke[6],
E. Meninno[29,114], M. Meres[13], S. Mhlanga[124], Y. Miake[133], L. Micheletti[25], L.C. Migliorin[135],
D.L. Mihaylov[105], K. Mikhaylov[75,92], A.N. Mishra[69], D. Miśkowiec[107], A. Modak[3],
N. Mohammadi[34], A.P. Mohanty[63], B. Mohanty[86], M. Mohisin Khan[16,v], Z. Moravcova[89],
C. Mordasini[105], D.A. Moreira De Godoy[144], L.A.P. Moreno[45], I. Morozov[62], A. Morsch[34],
T. Mrnjavac[34], V. Muccifora[52], E. Mudnic[35], D. Mühlheim[144], S. Muhuri[141], J.D. Mulligan[80],
M.G. Munhoz[121], R.H. Munzer[68], H. Murakami[132], S. Murray[124], L. Musa[34], J. Musinsky[64],
C.J. Myers[125], J.W. Myrcha[142], B. Naik[49], R. Nair[85], B.K. Nandi[49], R. Nania[10,54], E. Nappi[53],
M.U. Naru[14], A.F. Nassirpour[81], C. Nattrass[130], R. Nayak[49], T.K. Nayak[86], S. Nazarenko[109],
A. Neagu[20], R.A. Negrao De Oliveira[68], L. Nellen[69], S.V. Nesbo[36], G. Neskovic[39], D. Nesterov[113],
L.T. Neumann[142], B.S. Nielsen[89], S. Nikolaev[88], S. Nikulin[88], V. Nikulin[98], F. Noferini[10,54],
P. Nomokonov[75], J. Norman[79,127], N. Novitzky[133], P. Nowakowski[142], A. Nyanin[88],
J. Nystrand[21], M. Ogino[82], A. Ohlson[81,104], J. Oleniacz[142], A.C. Oliveira Da Silva[130],
M.H. Oliver[146], C. Oppedisano[59], A. Ortiz Velasquez[69], A. Oskarsson[81], J. Otwinowski[118],
K. Oyama[82], Y. Pachmayer[104], V. Pacik[89], D. Pagano[140], G. Paić[69], J. Pan[143], S. Panebianco[137],
P. Pareek[50,141], J. Park[61], J.E. Parkkila[126], S. Parmar[100], S.P. Pathak[125], B. Paul[23], H. Pei[6],
T. Peitzmann[63], X. Peng[6], L.G. Pereira[70], H. Pereira Da Costa[137], D. Peresunko[88], G.M. Perez[8],
Y. Pestov[4], V. Petráček[37], M. Petrovici[48], R.P. Pezzi[70], S. Piano[60], M. Pikna[13], P. Pillot[115],
O. Pinazza[34,54], L. Pinsky[125], C. Pinto[27], S. Pisano[10,52], D. Pistone[56], M. Płoskoń[80],
M. Planinic[99], F. Pliquett[68], M.G. Poghosyan[96], B. Polichtchouk[91], N. Poljak[99], A. Pop[48],
S. Porteboeuf-Houssais[134], V. Pozdniakov[75], S.K. Prasad[3], R. Preghenella[54], F. Prino[59],
C.A. Pruneau[143], I. Pshenichnov[62], M. Puccio[34], J. Putschke[143], L. Quaglia[25], R.E. Quishpe[125],
S. Ragoni[111], S. Raha[3], S. Rajput[101], J. Rak[126], A. Rakotozafindrabe[137], L. Ramello[31],
F. Rami[136], S.A.R. Ramirez[45], R. Raniwala[102], S. Raniwala[102], S.S. Räsänen[44], R. Rath[50],
V. Ratza[43], I. Ravasenga[90], K.F. Read[96,130], A.R. Redelbach[39], K. Redlich[85,vi], A. Rehman[21],
P. Reichelt[68], F. Reidt[34], X. Ren[6], R. Renfordt[68], Z. Rescakova[38], K. Reygers[104], V. Riabov[98],
T. Richert[81,89], M. Richter[20], P. Riedler[34], W. Riegler[34], F. Riggi[27], C. Ristea[67], S.P. Rode[50],
M. Rodríguez Cahuantzi[45], K. Røed[20], R. Rogalev[91], E. Rogochaya[75], D. Rohr[34], D. Röhrich[21],
P.S. Rokita[142], F. Ronchetti[52], A. Rosano[56], E.D. Rosas[69], K. Roslon[142], A. Rossi[28,57],
A. Rotondi[139], A. Roy[50], P. Roy[110], O.V. Rueda[81], R. Rui[24], B. Rumyantsev[75], A. Rustamov[87],
E. Ryabinkin[88], Y. Ryabov[98], A. Rybicki[118], H. Rytkonen[126], O.A.M. Saarimaki[44], S. Sadhu[141],
S. Sadovsky[91], K. Šafařík[37], S.K. Saha[141], B. Sahoo[49], P. Sahoo[49], R. Sahoo[50], S. Sahoo[65],
P.K. Sahu[65], J. Saini[141], S. Sakai[133], S. Sambyal[101], V. Samsonov[93,98], D. Sarkar[143], N. Sarkar[141],
P. Sarma[42], V.M. Sarti[105], M.H.P. Sas[63], E. Scapparone[54], J. Schambach[119], H.S. Scheid[68],
C. Schiaua[48], R. Schicker[104], A. Schmah[104], C. Schmidt[107], H.R. Schmidt[103], M.O. Schmidt[104],
M. Schmidt[103], N.V. Schmidt[68,96], A.R. Schmier[130], J. Schukraft[89], Y. Schutz[34,136],
K. Schwarz[107], K. Schweda[107], G. Scioli[26], E. Scomparin[59], M. Šefčík[38], J.E. Seger[15],
Y. Sekiguchi[132], D. Sekihata[132], I. Selyuzhenkov[93,107], S. Senyukov[136], D. Serebryakov[62],
A. Sevcenco[67], A. Shabanov[62], A. Shabetai[115], R. Shahoyan[34], W. Shaikh[110], A. Shangaraev[91],
A. Sharma[100], A. Sharma[101], H. Sharma[118], M. Sharma[101], N. Sharma[100], S. Sharma[101],
A.I. Sheikh[141], K. Shigaki[46], M. Shimomura[83], S. Shirinkin[92], Q. Shou[40], Y. Sibiriak[88],
S. Siddhanta[55], T. Siemiarczuk[85], D. Silvermyr[81], G. Simatovic[90], G. Simonetti[34], B. Singh[105],
R. Singh[86], R. Singh[101], R. Singh[50], V.K. Singh[141], V. Singhal[141], T. Sinha[110], B. Sitar[13],
M. Sitta[31], T.B. Skaali[20], M. Slupecki[126], N. Smirnov[146], R.J.M. Snellings[63], C. Soncco[112],
J. Song[125], A. Songmoolnak[116], F. Soramel[28], S. Sorensen[130], I. Sputowska[118], J. Stachel[104],

I. Stan[67], P. Stankus[96], P.J. Steffanic[130], E. Stenlund[81], D. Stocco[115], M.M. Storetvedt[36], L.D. Stritto[29], A.A.P. Suaide[121], T. Sugitate[46], C. Suire[78], M. Suleymanov[14], M. Suljic[34], R. Sultanov[92], M. Šumbera[95], V. Sumberia[101], S. Sumowidagdo[51], S. Swain[65], A. Szabo[13], I. Szarka[13], U. Tabassam[14], S.F. Taghavi[105], G. Taillepied[134], J. Takahashi[122], G.J. Tambave[21], S. Tang[6,134], M. Tarhini[115], M.G. Tarzila[48], A. Tauro[34], G. Tejeda Muñoz[45], A. Telesca[34], L. Terlizzi[25], C. Terrevoli[125], D. Thakur[50], S. Thakur[141], D. Thomas[119], F. Thoresen[89], R. Tieulent[135], A. Tikhonov[62], A.R. Timmins[125], A. Toia[68], N. Topilskaya[62], M. Toppi[52], F. Torales-Acosta[19], S.R. Torres[37,120], A. Trifiró[32,56], S. Tripathy[50,69], T. Tripathy[49], S. Trogolo[28], G. Trombetta[33], L. Tropp[38], V. Trubnikov[2], W.H. Trzaska[126], T.P. Trzcinski[142], B.A. Trzeciak[37,63], A. Tumkin[109], R. Turrisi[57], T.S. Tveter[20], K. Ullaland[21], E.N. Umaka[125], A. Uras[135], G.L. Usai[23], M. Vala[38], N. Valle[139], S. Vallero[59], N. van der Kolk[63], L.V.R. van Doremalen[63], M. van Leeuwen[63], P. Vande Vyvre[34], D. Varga[145], Z. Varga[145], M. Varga-Kofarago[145], A. Vargas[45], M. Vasileiou[84], A. Vasiliev[88], O. Vázquez Doce[105], V. Vechernin[113], E. Vercellin[25], S. Vergara Limón[45], L. Vermunt[63], R. Vernet[7], R. Vértesi[145], L. Vickovic[35], Z. Vilakazi[131], O. Villalobos Baillie[111], G. Vino[53], A. Vinogradov[88], T. Virgili[29], V. Vislavicius[89], A. Vodopyanov[75], B. Volkel[34], M.A. Völkl[103], K. Voloshin[92], S.A. Voloshin[143], G. Volpe[33], B. von Haller[34], I. Vorobyev[105], D. Voscek[117], J. Vrláková[38], B. Wagner[21], M. Weber[114], A. Wegrzynek[34], S.C. Wenzel[34], J.P. Wessels[144], J. Wiechula[68], J. Wikne[20], G. Wilk[85], J. Wilkinson[10,54], G.A. Willems[144], E. Willsher[111], B. Windelband[104], M. Winn[137], W.E. Witt[130], Y. Wu[128], R. Xu[6], S. Yalcin[77], Y. Yamaguchi[46], K. Yamakawa[46], S. Yang[21], S. Yano[137], Z. Yin[6], H. Yokoyama[63], I.-K. Yoo[17], J.H. Yoon[61], S. Yuan[21], A. Yuncu[104], V. Yurchenko[2], V. Zaccolo[24], A. Zaman[14], C. Zampolli[34], H.J.C. Zanoli[63], N. Zardoshti[34], A. Zarochentsev[113], P. Závada[66], N. Zaviyalov[109], H. Zbroszczyk[142], M. Zhalov[98], S. Zhang[40], X. Zhang[6], Z. Zhang[6], V. Zherebchevskii[113], D. Zhou[6], Y. Zhou[89], Z. Zhou[21], J. Zhu[6,107], Y. Zhu[6], A. Zichichi[10,26], G. Zinovjev[2], N. Zurlo[140],

[i] *Deceased*

[ii] *Italian National Agency for New Technologies, Energy and Sustainable Economic Development (ENEA), Bologna, Italy*

[iii] *Dipartimento DET del Politecnico di Torino, Turin, Italy*

[iv] *M.V. Lomonosov Moscow State University, D.V. Skobeltsyn Institute of Nuclear, Physics, Moscow, Russia*

[v] *Department of Applied Physics, Aligarh Muslim University, Aligarh, India*

[vi] *Institute of Theoretical Physics, University of Wroclaw, Poland*

[1] *A.I. Alikhanyan National Science Laboratory (Yerevan Physics Institute) Foundation, Yerevan, Armenia*

[2] *Bogolyubov Institute for Theoretical Physics, National Academy of Sciences of Ukraine, Kiev, Ukraine*

[3] *Bose Institute, Department of Physics and Centre for Astroparticle Physics and Space Science (CAPSS), Kolkata, India*

[4] *Budker Institute for Nuclear Physics, Novosibirsk, Russia*

[5] *California Polytechnic State University, San Luis Obispo, California, United States*

[6] *Central China Normal University, Wuhan, China*

[7] *Centre de Calcul de l'IN2P3, Villeurbanne, Lyon, France*

[8] *Centro de Aplicaciones Tecnológicas y Desarrollo Nuclear (CEADEN), Havana, Cuba*

[9] *Centro de Investigación y de Estudios Avanzados (CINVESTAV), Mexico City and Mérida, Mexico*

[10] *Centro Fermi - Museo Storico della Fisica e Centro Studi e Ricerche "Enrico Fermi', Rome, Italy*

[11] *Chicago State University, Chicago, Illinois, United States*

12 *China Institute of Atomic Energy, Beijing, China*

13 *Comenius University Bratislava, Faculty of Mathematics, Physics and Informatics, Bratislava, Slovakia*

14 *COMSATS University Islamabad, Islamabad, Pakistan*

15 *Creighton University, Omaha, Nebraska, United States*

16 *Department of Physics, Aligarh Muslim University, Aligarh, India*

17 *Department of Physics, Pusan National University, Pusan, Republic of Korea*

18 *Department of Physics, Sejong University, Seoul, Republic of Korea*

19 *Department of Physics, University of California, Berkeley, California, United States*

20 *Department of Physics, University of Oslo, Oslo, Norway*

21 *Department of Physics and Technology, University of Bergen, Bergen, Norway*

22 *Dipartimento di Fisica dell'Università 'La Sapienza' and Sezione INFN, Rome, Italy*

23 *Dipartimento di Fisica dell'Università and Sezione INFN, Cagliari, Italy*

24 *Dipartimento di Fisica dell'Università and Sezione INFN, Trieste, Italy*

25 *Dipartimento di Fisica dell'Università and Sezione INFN, Turin, Italy*

26 *Dipartimento di Fisica e Astronomia dell'Università and Sezione INFN, Bologna, Italy*

27 *Dipartimento di Fisica e Astronomia dell'Università and Sezione INFN, Catania, Italy*

28 *Dipartimento di Fisica e Astronomia dell'Università and Sezione INFN, Padova, Italy*

29 *Dipartimento di Fisica 'E.R. Caianiello' dell'Università and Gruppo Collegato INFN, Salerno, Italy*

30 *Dipartimento DISAT del Politecnico and Sezione INFN, Turin, Italy*

31 *Dipartimento di Scienze e Innovazione Tecnologica dell'Università del Piemonte Orientale and INFN Sezione di Torino, Alessandria, Italy*

32 *Dipartimento di Scienze MIFT, Università di Messina, Messina, Italy*

33 *Dipartimento Interateneo di Fisica 'M. Merlin' and Sezione INFN, Bari, Italy*

34 *European Organization for Nuclear Research (CERN), Geneva, Switzerland*

35 *Faculty of Electrical Engineering, Mechanical Engineering and Naval Architecture, University of Split, Split, Croatia*

36 *Faculty of Engineering and Science, Western Norway University of Applied Sciences, Bergen, Norway*

37 *Faculty of Nuclear Sciences and Physical Engineering, Czech Technical University in Prague, Prague, Czech Republic*

38 *Faculty of Science, P.J. Šafárik University, Košice, Slovakia*

39 *Frankfurt Institute for Advanced Studies, Johann Wolfgang Goethe-Universität Frankfurt, Frankfurt, Germany*

40 *Fudan University, Shanghai, China*

41 *Gangneung-Wonju National University, Gangneung, Republic of Korea*

42 *Gauhati University, Department of Physics, Guwahati, India*

43 *Helmholtz-Institut für Strahlen- und Kernphysik, Rheinische Friedrich-Wilhelms-Universität Bonn, Bonn, Germany*

44 *Helsinki Institute of Physics (HIP), Helsinki, Finland*

45 *High Energy Physics Group, Universidad Autónoma de Puebla, Puebla, Mexico*

46 *Hiroshima University, Hiroshima, Japan*

47 *Hochschule Worms, Zentrum für Technologietransfer und Telekommunikation (ZTT), Worms, Germany*

48 *Horia Hulubei National Institute of Physics and Nuclear Engineering, Bucharest, Romania*

49 *Indian Institute of Technology Bombay (IIT), Mumbai, India*

50 *Indian Institute of Technology Indore, Indore, India*

51 *Indonesian Institute of Sciences, Jakarta, Indonesia*

52 *INFN, Laboratori Nazionali di Frascati, Frascati, Italy*

53 *INFN, Sezione di Bari, Bari, Italy*

54 *INFN, Sezione di Bologna, Bologna, Italy*

55 *INFN, Sezione di Cagliari, Cagliari, Italy*

56 *INFN, Sezione di Catania, Catania, Italy*
57 *INFN, Sezione di Padova, Padova, Italy*
58 *INFN, Sezione di Roma, Rome, Italy*
59 *INFN, Sezione di Torino, Turin, Italy*
60 *INFN, Sezione di Trieste, Trieste, Italy*
61 *Inha University, Incheon, Republic of Korea*
62 *Institute for Nuclear Research, Academy of Sciences, Moscow, Russia*
63 *Institute for Subatomic Physics, Utrecht University/Nikhef, Utrecht, Netherlands*
64 *Institute of Experimental Physics, Slovak Academy of Sciences, Košice, Slovakia*
65 *Institute of Physics, Homi Bhabha National Institute, Bhubaneswar, India*
66 *Institute of Physics of the Czech Academy of Sciences, Prague, Czech Republic*
67 *Institute of Space Science (ISS), Bucharest, Romania*
68 *Institut für Kernphysik, Johann Wolfgang Goethe-Universität Frankfurt, Frankfurt, Germany*
69 *Instituto de Ciencias Nucleares, Universidad Nacional Autónoma de México, Mexico City, Mexico*
70 *Instituto de Física, Universidade Federal do Rio Grande do Sul (UFRGS), Porto Alegre, Brazil*
71 *Instituto de Física, Universidad Nacional Autónoma de México, Mexico City, Mexico*
72 *iThemba LABS, National Research Foundation, Somerset West, South Africa*
73 *Jeonbuk National University, Jeonju, Republic of Korea*
74 *Johann-Wolfgang-Goethe Universität Frankfurt Institut für Informatik, Fachbereich Informatik und Mathematik, Frankfurt, Germany*
75 *Joint Institute for Nuclear Research (JINR), Dubna, Russia*
76 *Korea Institute of Science and Technology Information, Daejeon, Republic of Korea*
77 *KTO Karatay University, Konya, Turkey*
78 *Laboratoire de Physique des 2 Infinis, Irène Joliot-Curie, Orsay, France*
79 *Laboratoire de Physique Subatomique et de Cosmologie, Université Grenoble-Alpes, CNRS-IN2P3, Grenoble, France*
80 *Lawrence Berkeley National Laboratory, Berkeley, California, United States*
81 *Lund University Department of Physics, Division of Particle Physics, Lund, Sweden*
82 *Nagasaki Institute of Applied Science, Nagasaki, Japan*
83 *Nara Women's University (NWU), Nara, Japan*
84 *National and Kapodistrian University of Athens, School of Science, Department of Physics , Athens, Greece*
85 *National Centre for Nuclear Research, Warsaw, Poland*
86 *National Institute of Science Education and Research, Homi Bhabha National Institute, Jatni, India*
87 *National Nuclear Research Center, Baku, Azerbaijan*
88 *National Research Centre Kurchatov Institute, Moscow, Russia*
89 *Niels Bohr Institute, University of Copenhagen, Copenhagen, Denmark*
90 *Nikhef, National institute for subatomic physics, Amsterdam, Netherlands*
91 *NRC Kurchatov Institute IHEP, Protvino, Russia*
92 *NRC "Kurchatov Institute" - ITEP, Moscow, Russia*
93 *NRNU Moscow Engineering Physics Institute, Moscow, Russia*
94 *Nuclear Physics Group, STFC Daresbury Laboratory, Daresbury, United Kingdom*
95 *Nuclear Physics Institute of the Czech Academy of Sciences, Řež u Prahy, Czech Republic*
96 *Oak Ridge National Laboratory, Oak Ridge, Tennessee, United States*
97 *Ohio State University, Columbus, Ohio, United States*
98 *Petersburg Nuclear Physics Institute, Gatchina, Russia*
99 *Physics department, Faculty of science, University of Zagreb, Zagreb, Croatia*
100 *Physics Department, Panjab University, Chandigarh, India*
101 *Physics Department, University of Jammu, Jammu, India*
102 *Physics Department, University of Rajasthan, Jaipur, India*
103 *Physikalisches Institut, Eberhard-Karls-Universität Tübingen, Tübingen, Germany*
104 *Physikalisches Institut, Ruprecht-Karls-Universität Heidelberg, Heidelberg, Germany*

[105] *Physik Department, Technische Universität München, Munich, Germany*
[106] *Politecnico di Bari, Bari, Italy*
[107] *Research Division and ExtreMe Matter Institute EMMI, GSI Helmholtzzentrum für Schwerionenforschung GmbH, Darmstadt, Germany*
[108] *Rudjer Bošković Institute, Zagreb, Croatia*
[109] *Russian Federal Nuclear Center (VNIIEF), Sarov, Russia*
[110] *Saha Institute of Nuclear Physics, Homi Bhabha National Institute, Kolkata, India*
[111] *School of Physics and Astronomy, University of Birmingham, Birmingham, United Kingdom*
[112] *Sección Física, Departamento de Ciencias, Pontificia Universidad Católica del Perú, Lima, Peru*
[113] *St. Petersburg State University, St. Petersburg, Russia*
[114] *Stefan Meyer Institut für Subatomare Physik (SMI), Vienna, Austria*
[115] *SUBATECH, IMT Atlantique, Université de Nantes, CNRS-IN2P3, Nantes, France*
[116] *Suranaree University of Technology, Nakhon Ratchasima, Thailand*
[117] *Technical University of Košice, Košice, Slovakia*
[118] *The Henryk Niewodniczanski Institute of Nuclear Physics, Polish Academy of Sciences, Cracow, Poland*
[119] *The University of Texas at Austin, Austin, Texas, United States*
[120] *Universidad Autónoma de Sinaloa, Culiacán, Mexico*
[121] *Universidade de São Paulo (USP), São Paulo, Brazil*
[122] *Universidade Estadual de Campinas (UNICAMP), Campinas, Brazil*
[123] *Universidade Federal do ABC, Santo Andre, Brazil*
[124] *University of Cape Town, Cape Town, South Africa*
[125] *University of Houston, Houston, Texas, United States*
[126] *University of Jyväskylä, Jyväskylä, Finland*
[127] *University of Liverpool, Liverpool, United Kingdom*
[128] *University of Science and Technology of China, Hefei, China*
[129] *University of South-Eastern Norway, Tonsberg, Norway*
[130] *University of Tennessee, Knoxville, Tennessee, United States*
[131] *University of the Witwatersrand, Johannesburg, South Africa*
[132] *University of Tokyo, Tokyo, Japan*
[133] *University of Tsukuba, Tsukuba, Japan*
[134] *Université Clermont Auvergne, CNRS/IN2P3, LPC, Clermont-Ferrand, France*
[135] *Université de Lyon, Université Lyon 1, CNRS/IN2P3, IPN-Lyon, Villeurbanne, Lyon, France*
[136] *Université de Strasbourg, CNRS, IPHC UMR 7178, F-67000 Strasbourg, France, Strasbourg, France*
[137] *Université Paris-Saclay Centre d'Etudes de Saclay (CEA), IRFU, Départment de Physique Nucléaire (DPhN), Saclay, France*
[138] *Università degli Studi di Foggia, Foggia, Italy*
[139] *Università degli Studi di Pavia, Pavia, Italy*
[140] *Università di Brescia, Brescia, Italy*
[141] *Variable Energy Cyclotron Centre, Homi Bhabha National Institute, Kolkata, India*
[142] *Warsaw University of Technology, Warsaw, Poland*
[143] *Wayne State University, Detroit, Michigan, United States*
[144] *Westfälische Wilhelms-Universität Münster, Institut für Kernphysik, Münster, Germany*
[145] *Wigner Research Centre for Physics, Budapest, Hungary*
[146] *Yale University, New Haven, Connecticut, United States*
[147] *Yonsei University, Seoul, Republic of Korea*